6-90-63-68 • OCTOBER 1963

6-90-63-68

TECHNICAL REPORT: COMMUNICATIONS

APPLICATION OF DELAY-LOCK RADAR TECHNIQUES TO DEEP SPACE TASKS

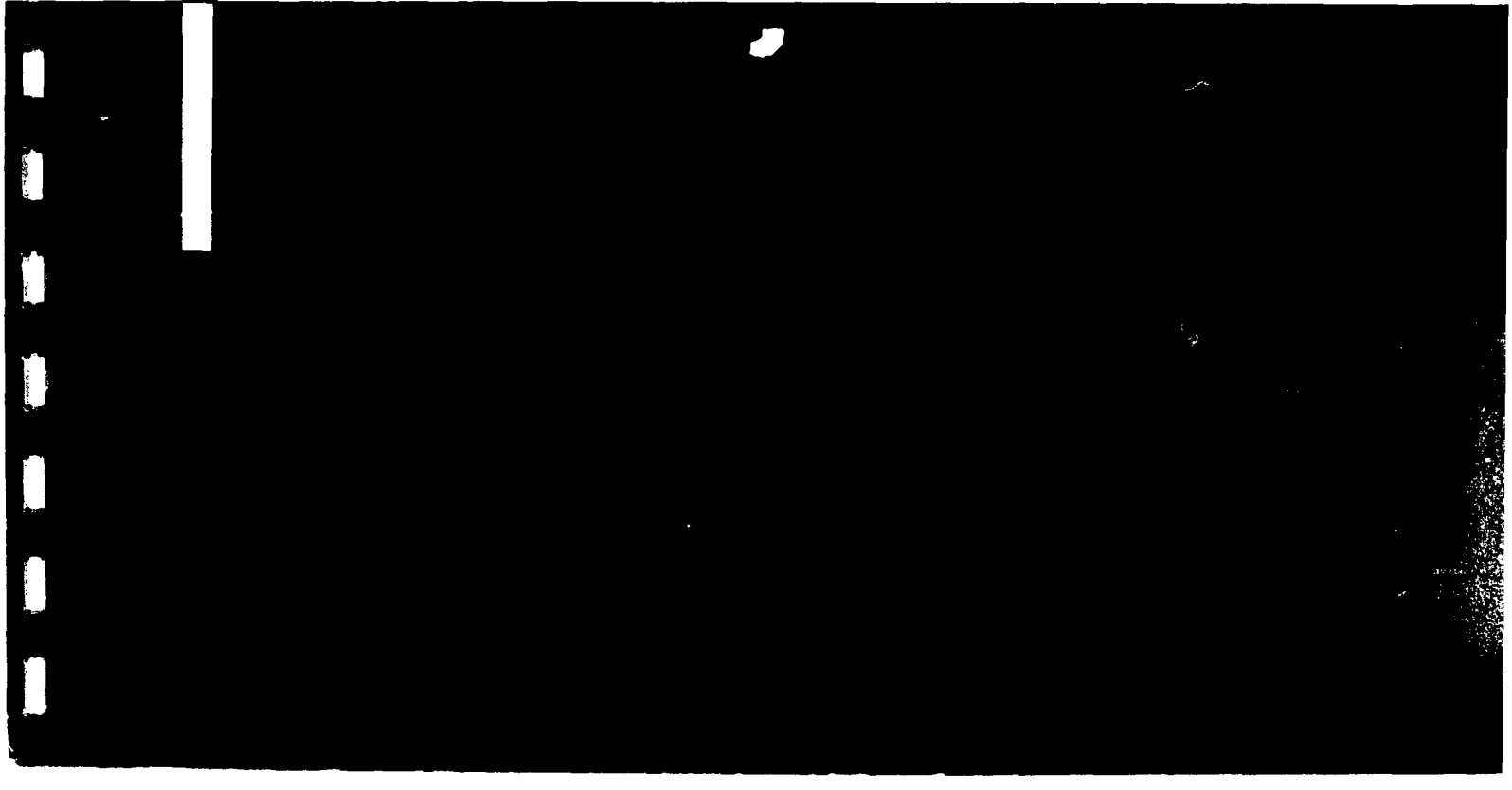

NOTICE

QUALIFIED REQUESTERS MAY OBTAIN COPIES OF THIS REPORT FROM THE DEFENSE DOCUMENTATION CENTER (DDC). DEPARTMENT OF DEFENSE CONTRACTORS MUST BE ESTABLISHED FOR DDC SERVICES. OR HAVE THEIR NEED-TO-KNOW CERTIFIED BY THE MILITARY AGENCY COGNIZANT OF THEIR CONTRACT.

COPIES OF THIS REPORT MAY BE OBTAINED FROM THE OFFICE OF TECHNICAL SERVICES. DEPARTMENT OF COMMERCE. WASHINGTON 25. D.C.

DISTRIBUTION OF THIS REPORT TO OTHERS SHALL NOT BE CONSTRUED AS GRANTING OR IMPLYING A LICENSE TO MAKE. USE. OR SELL ANY INVENTION DESCRIBED HEREIN UPON WHICH A PATENT HAS BEEN GRANTED OR A PATENT APPLICATION FILED BY LOCKHEED AIRCRAFT CORPORATION. NO LIABILITY IS ASSUMED BY LOCKHEED AS TO INFRINGEMENT OF PATENTS OWNED BY OTHERS.

WORK CARRIED OUT AS PART OF THE LOCKHEED INDEPENDENT RESEARCH PROGRAM.

6-90-63-68 • OCTOBER 1963

6-90-63-68

TECHNICAL REPORT: COMMUNICATIONS

APPLICATION OF DELAY-LOCK RADAR TECHNIQUES TO DEEP SPACE TASKS

by

R. B. WARD

WORK CARRIED OUT AS PART OF THE LOCKHEED INDEPENDENT RESEARCH PROGRAM

Lockheed

MISSILES & SPACE COMPANY

A GROUP DIVISION OF LOCKHEED AIRCRAFT CORPORATION

SUNNYVALE, CALIFORNIA

NOTICE

QUALIFIED REQUESTERS MAY OBTAIN COPIES OF THIS REPORT FROM THE DEFENSE DOCUMENTATION CENTER (DDC). DEPARTMENT OF DEFENSE CONTRACTORS MUST BE ESTABLISHED FOR DDC SERVICES. OR HAVE THEIR NEED-TO-KNOW CERTIFIED BY THE MILITARY AGENCY COGNIZANT OF THEIR CONTRACT.

COPIES OF THIS REPORT MAY BE OBTAINED FROM THE OFFICE OF TECHNICAL SERVICES. DEPARTMENT OF COMMERCE. WASHINGTON 25. D.C.

DISTRIBUTION OF THIS REPORT TO OTHERS SHALL NOT BE CONSTRUED AS GRANTING OR IMPLYING A LICENSE TO MAKE. USE. OR SELL ANY INVENTION DESCRIBED HEREIN UPON WHICH A PATENT HAS BEEN GRANTED OR A PATENT APPLICATION FILED BY LOCKHEED AIRCRAFT CORPORATION. NO LIABILITY IS ASSUMED BY LOCKHEED AS TO INFRINGEMENT OF PATENTS OWNED BY OTHERS.

SUMMARY

This report discusses the use of delay-lock radar techniques for deep-space tracking and communications tasks. To illustrate these techniques, a Mars or Venus space probe of the Voyager type is used as a typical mission. The Voyager is an unmanned vehicle in the 6,000-lb class which is planned for scientific and exploratory purposes from the years 1967 to 1975.

A brief introduction to the results of delay-lock radar development to date is given, followed by a description of the digital delay-lock discriminator. A discussion is then given on the problems inherent in the modulation and demodulation which is required to make full use of the delay-lock capability.

An integrated delay-lock two-way tracking-communications system suitable for the assumed mission is then described and the performance to be expected is calculated. This anticipated performance indicates considerable improvement over present capabilities.

CONTENTS

ILLUSTRATIONS

NOTATION

a	spatial acceleration
a_d	delay acceleration (sec/sec^2)
B_F	bandwidth of the postcorrelation filter
B_{LF}	bandwidth after detection
B_n	noise bandwidth of a delay-lock loop $\triangleq \int_0^\infty \lvert H \rvert^2 d\omega$
B_{RF}	single-sided frequency predetection bandwidth
c	velocity of propagation
E	signal energy
f_c	clock frequency
f_d	frequency difference between transmitter clock and receiver clock
f_{IF}	intermediate frequency
G_{R1}	spacecraft command-antenna gain
G_{R2}	gain of the earth receiving antenna
G_{T1}	gain of the earth transmitting antenna
G_{T2}	spacecraft high-gain antenna gain
k	Boltzmann's constant
N_o	double-sided noise power spectral density
n	number of stages in the sequence generator
$P( )$	probability that
P_N	noise power
P_R	received power

P_S	signal power
P_{T1}	earth transmitter power, average
P_{T2}	spacecraft transmitter power, average
p	complex frequency variable
p_o	loop-filter frequency constant
R	range, earth to spacecraft
R_{max}	maximum range of operation
$\dot{R}$	range rate
$\dot{R}_{max}$	maximum range rate
$\ddot{R}_{max}$	maximum acceleration
S	distance between antenna phase centers
SNR_d	signal-to-noise ratio (SNR) in the RF bandwidth, predetection
SNR_i	SNR at the input to the delay-lock loop
SNR_o	SNR at the output of a delay-lock loop
SNR_p	SNR at the input of the pulse rectifier
$\hat{T}$	estimate of time delay
$T_{a,max}$	maximum acquisition time
T_S	duration of pseudorandom sequence
T_1	spacecraft receiver, effective noise temperature
T_2	earth receiver, effective noise temperature
t	time variable
$\bar{u}$	mean value of the cross correlation of signal plus noise with the signal
$\dot{y}$	normalized delay-search velocity
Δ	period of the sequence generator clock

δ	integration time of integrate-and-dump bit decision process
ϵ	time difference between a received sequence and a local sequence at the n - 1 sequence generator tap
ϵ_{SS}	steady-state delay error
θ	angle to the target, measured from the midpoint of the antenna baseline
λ_1	wavelength, earth-to-spacecraft carrier
λ_2	wavelength, spacecraft-to-earth carrier
σ_T^2	variance of the time-delay measurement
$\sigma_{Td\ell}$	root mean square (rms) delay error
σ_θ	rms angular error
σ_y	rms value of a variable y

Section 1
INTRODUCTION

1.1 BACKGROUND OF DELAY-LOCK RESEARCH

As described by Spilker and Magill, the delay-lock discriminator is a type of correlating circuit which tracks the time-delay between a locally generated, arbitrary signal and the same signal after it is delayed by some process such as transmission to and return from a target (Ref. 1). In the original paper, the tracking loop filter is optimized in the sense that the sum of the mean-squared noise error and the infinite-time integral of the transient error to a step of delay rate is minimized.

The delay-lock discriminator error characteristic is the function which relates open-loop error voltage to static delay error. This characteristic is essentially the derivative of the autocorrelation function of the transmitted signal (Ref. 2). Therefore, to avoid ambiguities in delay, the spectrum of the transmitted signal should ideally be low pass. Such a signal could be generated by a random process. However, other signals whose spectra do not extend quite to zero frequency are also suitable because the ambiguities in delay are widely separated. A particular case of this sort is the maximal-length binary sequence.

Delay-lock tracking of binary sequences has been treated by Spilker in Ref. 3. One of the main advantages of such a signal is the simplification it permits in the delay-lock circuitry. Wide-bandwidth, variable-delay, high-accuracy delay elements having long delays are not required and analog multiplication of voltages can be replaced by modulo 2 addition.

O'Sullivan considers the application of the analog delay-lock discriminator to satellite range and angle-tracking in Ref. 2. Weiss and Evans discuss the use of a digital delay-lock discriminator in a satellite-rendezvous radar. See Ref. 4.

1.2 DIGITAL DELAY-LOCK DISCRIMINATOR

A block diagram of a digital delay-lock loop is shown in Fig. 1-1. The feedback shift-register consists of n flip flops in series. Taps are taken from the outputs of appropriate stages and fed back to the input through a modulo 2 adder. This produces a linear maximal-length sequence at the shift register output whose length is $2^n - 1$ digits and whose duration is $(2^n - 1)\Delta$ sec, where Δ is the period of the clock. The same sequence appears at each of the shift-register taps, but it is advanced in time by Δ sec for each tap further from the output. The input sequence to the delay-lock loop is identical in form to the sequence generated by the feedback shift-register, but the input sequence time-of-arrival is arbitrary.

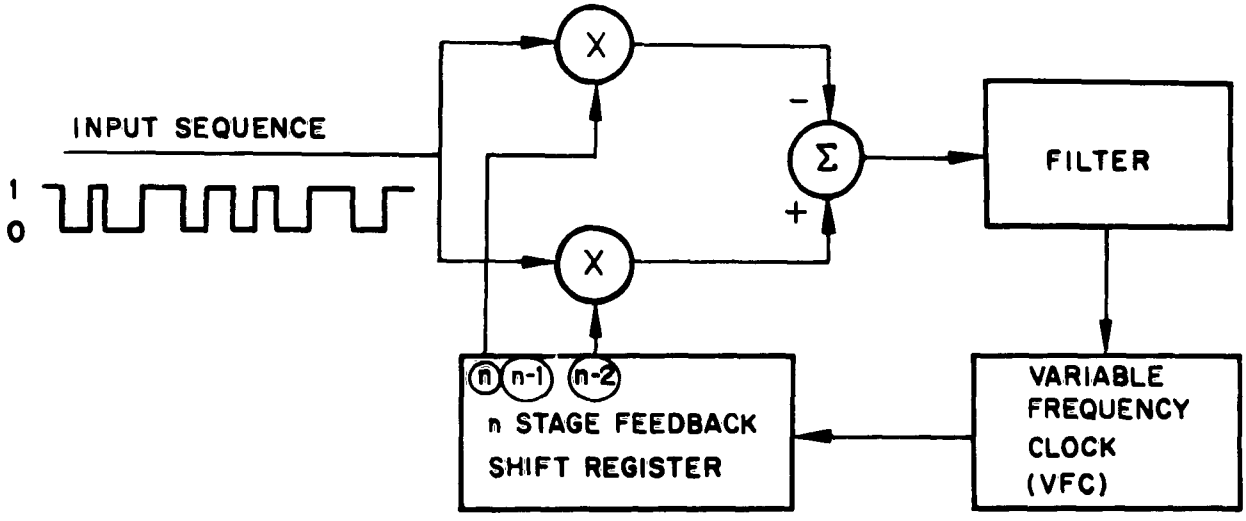

Fig. 1-1 Digital Delay-Lock Discriminator

The sequences may be thought to consist of 0's and 1's, and the operation 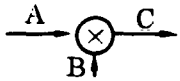 may be defined as modulo 2 addition; that is, $C \triangleq (A + \overline{B}) \cdot (\overline{A} + B)$.

Cross-correlations are thus performed between the input sequence and two local sequences separated by 2Δ. When the number of digits in the sequence is large,

the average output of each correlator as a function of delay error is as shown in Fig. 1-2.

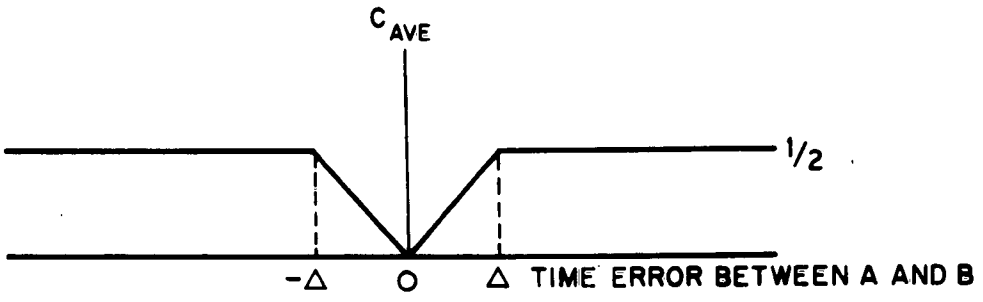

Fig. 1-2 Averaged Correlator Output

When the sequences are exactly synchronous, each pair of digits is identical and the output is always zero. When the sequences are displaced more than one digit, all four states of the input are equally probable and the correlator output averages one-half. Since the filter is low-pass, it obtains approximately the average of the differenced correlator outputs and produces the discriminator characteristic shown in Fig. 1-3.

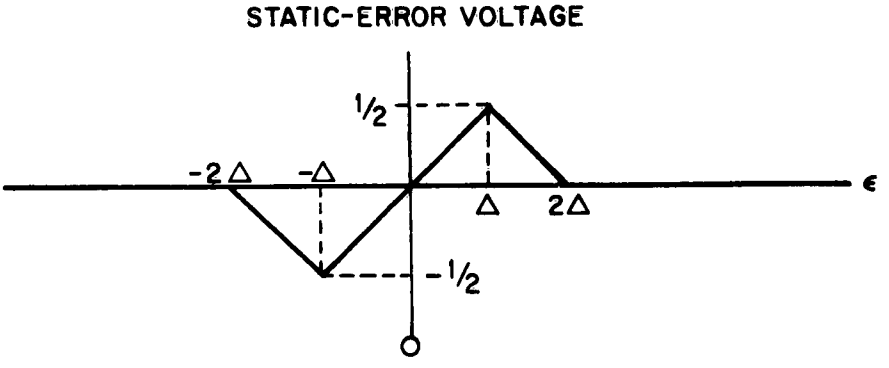

Fig. 1-3 Digital Delay-Lock Discriminator Curve

Here, ϵ is defined as the time difference between the input sequence and the sequence at the $n - 1$ shift-register tap. If the sequences are within $\pm 2\Delta$ of synchronism, an

error voltage exists. If the relative motion of the sequences is within certain bounds, the sequences lock in. The frequency of the voltage-controlled clock becomes the same as that of the input sequence clock, and the error, ϵ, is near zero. As long as noise or delay transients of the input sequence do not cause $|\epsilon| \geq 2\Delta$, the local sequence continues to track the input.

Section 2
SYSTEMS CONSIDERATIONS

2.1 BROADBAND CHARACTER OF DELAY-LOCK SIGNALS

The delay-lock system basically uses a broadband signal to either transmit or determine narrowband information. For example, a maximal-length binary sequence with a clock rate of 10 Mc might be used to determine delay variations having a bandwidth of 10 cps; or, modulation with a bit rate of 10 kc might be applied to the binary sequence. Although the binary sequence extends over a spectrum of approximately 10 Mc in these cases, the information bandwidth is much less. It is thus possible to retrieve the information even though the signal-to-noise ratio (SNR) in the bandwidth of the binary sequence is very small. In the examples given above, the delay-lock system provides information retrieval even though the SNR's are -50 and -20 db, respectively.

It is rarely possible to transmit directly a broadband low-pass signal. The typical situation requires that the low-pass signal be transformed to a bandpass signal for transmission. Many modulation-demodulation systems cause worsening of the SNR during demodulation if, at the demodulator input, the ratio is less than some threshold value (usually 0 to +20 db). Therefore, the modulation-demodulation system which is chosen must be appropriate for the particular problem.* For example, a short-range delay-lock system might employ amplitude modulation and envelope detection, and yet require only moderate transmitter power to maintain the input SNR greater than 0 db at the demodulator.

---

*It is possible to delay-lock track a bandpass signal without previous demodulation by delaying the transmitted bandpass signal for correlation with its return. This method, however, generates a fine structure of ambiguities in the delay-lock discriminator characteristic and usually requires delay lines that are not technically feasible at this time.

2.2 MODULATION SYSTEM FOR TYPICAL MARS MISSION

The two modulation systems chosen for the earth-spacecraft and spacecraft-earth links, respectively, are discussed in the following paragraphs. The earth-spacecraft link is illustrated in Fig. 2-1. On-off amplitude modulation is used at the transmitter and envelope detection is used at the spacecraft. This system was chosen because it is the simplest; it may be used because of the high transmitter power available and low command-bit rate.

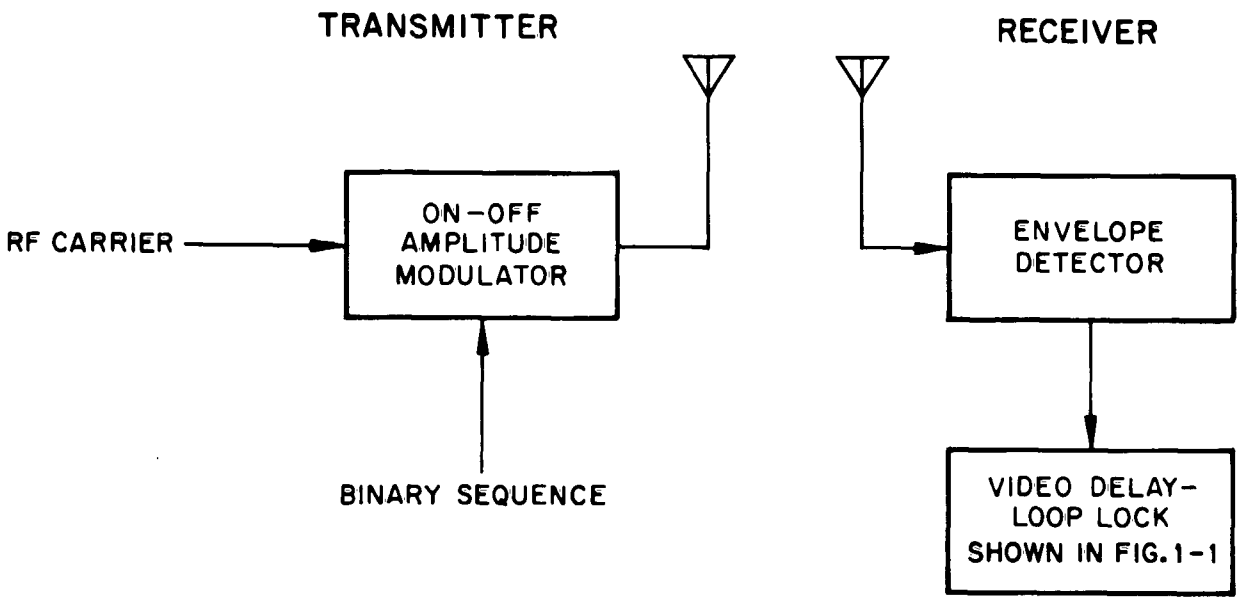

Fig. 2-1 Earth-to-Spacecraft Link

For the spacecraft-earth link, the transmitter power available is much less and the objective is to transmit at the highest possible data rate. To avoid degrading the data capability, synchronous transmission and demodulation are used. Synchronous demodulation does not change the SNR, so the full delay-lock capability is maintained.

One form of synchronous delay-lock tracking is illustrated in Fig. 2-2. At the transmitter, the RF carrier and the binary sequence are made to be synchronous. That is,

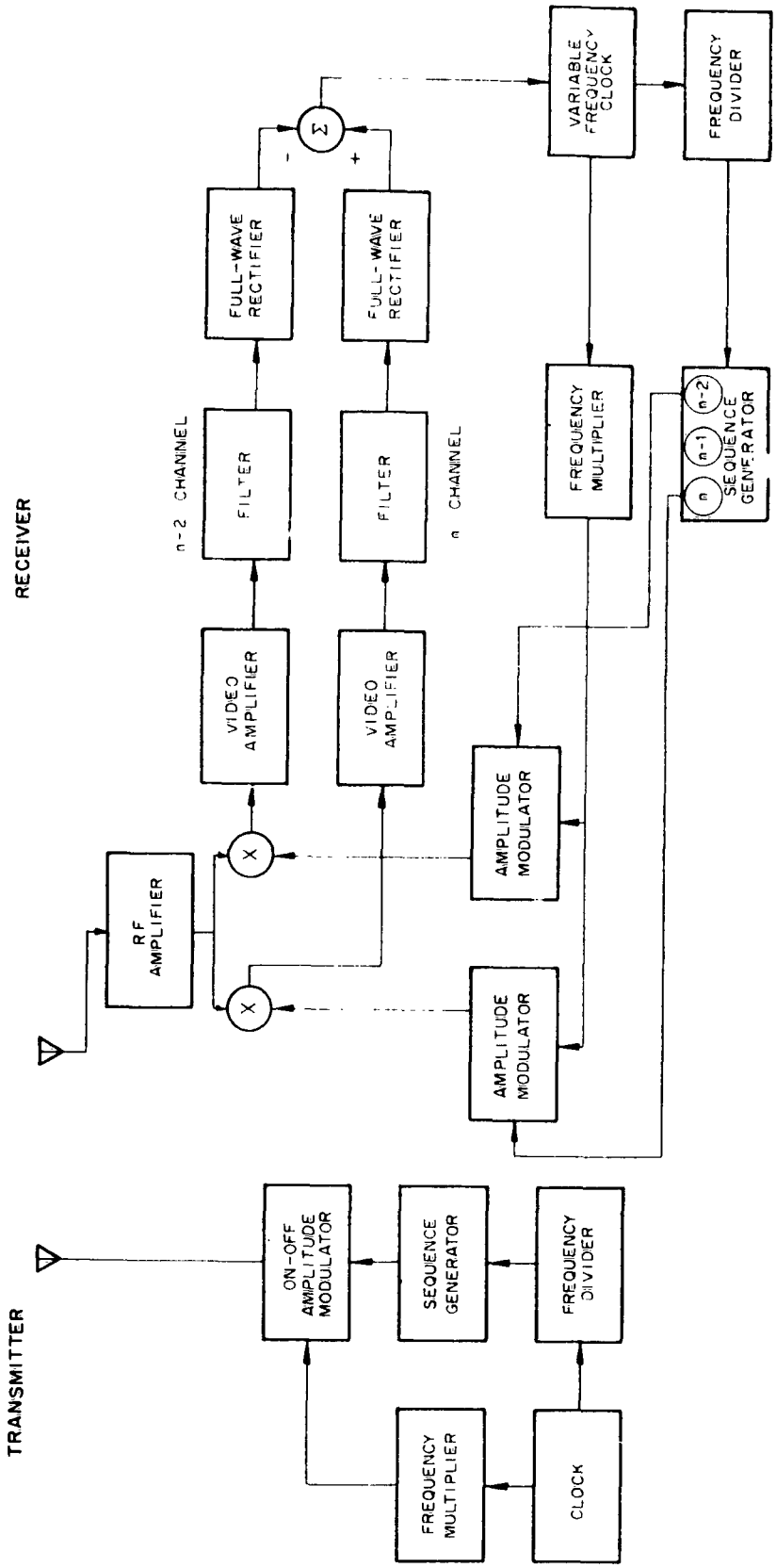

Fig. 2-2 Synchronous Delay-Lock System Using Amplitude Modulation

the signal which drives the sequence generator is derived by counting down from a master clock and the RF carrier is derived by frequency multiplication from the same master clock. The receiver contains a sequence generator, clock, frequency divider, and frequency multiplier; all of which are identical to those in the transmitter. The n and n - 2 taps of the sequence generator modulate the frequency-multiplier output so that two synchronous on-off modulated signals are obtained. Although the two signals are identical to the received signal, they are separated from each other by 2Δ. These two signals are used as references to synchronously detect and delay-lock track the incoming signal.

To illustrate the operation, consider that the variable-frequency clock is operating at exactly the same frequency as the incoming sequence, and the n-modulator output is in exact time synchronism with the incoming signal, including both the envelope and the carrier. The output of the n-channel synchronous detector will be the video sequence and consists of positive pulses that are present on the average of half of the time. Since there is no correlation at the n - 2 synchronous detector, positive pulses are present at its output on the average of one-quarter of the time. In each channel, the pulses are amplified and then passed through low-pass filters where the bandwidth is somewhat larger than the information and tracking bandwidths. The difference in the average voltage of the two channels is the peak delay-lock discriminator voltage as shown by Point 1 in Fig. 2-3.

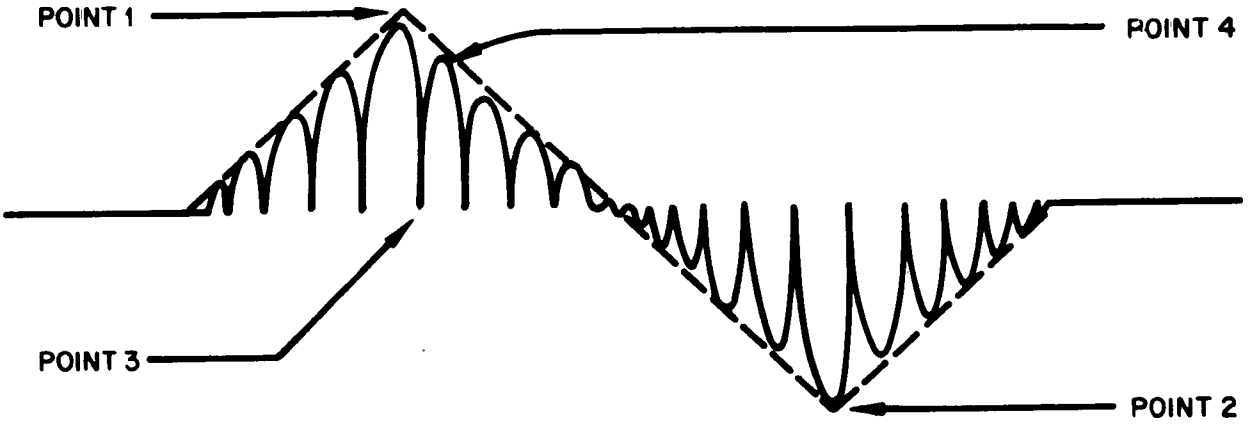

Fig. 2-3 Discriminator Characteristic of a Synchronous Delay-Lock System

If we now consider that the output of the n - 2 modulator is in time synchronism with the incoming signal, including both the envelope and the carrier, we find that the roles of the two channels are reversed. The difference in average voltage of the two channels has the opposite polarity and gives the second peak delay-lock discriminator voltage as shown by Point 2 in Fig. 2-3. As the delay is slowly varied from that of the first case, the most obvious effect is that a change occurs in the relative phase of the incoming RF carrier and the reference RF carrier. As the relative phase changes from 0 to 90 deg, the outputs of both synchronous detectors decrease from maximum positive pulses to zero and the discriminator error voltage likewise decreases to zero, as shown by Point 3 in Fig. 2-3. As the delay is further changed, the outputs of the synchronous detectors become negative pulses until, when the relative phase of the RF carriers is 180 deg, the negative pulses reach maximum amplitude. The reason for the full-wave rectifiers is now evident: the filtered negative pulses are reversed in sign so that the discriminator error voltage still has the correct polarity, as shown by Point 4 in Fig. 2-3. Since the only nonlinear operation (full-wave rectification) is performed after the bandwidth has been reduced, there is no degradation of the SNR.

The complete static delay-lock discriminator characteristic for the synchronous system (illustrated in Fig. 2-2) is shown in Fig. 2-3. The fine structure is due to variation of the RF carrier phase and the envelope is due to variation of the modulation-envelope phase. The polarity of the error voltage is always such as to reduce the error to zero and the system thus continues to track the incoming signal.

2.3 NOISE AND LOCK-ON PERFORMANCE

The discussion so far has assumed no noise. If noise is present, the error jitters about zero. Since the RF reference voltages are not locked directly to the incoming RF carrier, there may be some question regarding the system operation when a moderate amount of phase jitter occurs between the local clock and the incoming clock. Although frequency multiplication of the local clock may cause a phase difference of many cycles between the reference carrier and the incoming carrier, the full-wave rectifiers continue to provide the correct polarity of error signal. The limits of operation are reached when the spectrum of the phase-difference jitter becomes significantly wider than the video filter bandwidth. In this case, the filters do not pass the signals, and tracking ceases.

The method employed to obtain lock-on in a system of this type is very important. Because of the nature of the discriminator curve, the error voltage is zero for all delays greater than $\pm 2\Delta$; therefore, a search procedure is necessary. One method of search is to adjust the local-clock frequency so that it is slightly different from the incoming-clock frequency. This adjustment causes both a drift of the sequences and eventual lock-on when they come within $\pm 2\Delta$.

The difficulty with this simple scheme is that both the incoming carrier-frequency and the reference carrier-frequency must be maintained the same, within plus or minus the video-filter bandwidth. If the two carrier frequencies are not this close together, the outputs of the synchronous detectors contain no frequency components which can pass through the subsequent filters. Therefore, no error voltage can be produced to cause lock-on, even when the sequences sweep through synchronism. On the other hand, when the carrier frequencies are close enough, the frequency difference between the incoming sequence clock and the local sequence clock is often so small that for long sequences it may take a very long time, perhaps hours or days, for the sequences to reach synchronism.

An alternate method for lock-on is shown in the partial block diagram in Fig. 2-4. This method consists essentially of separating the time-search and frequency-search functions. Regardless of the relative delay of the sequences, an output is present from the full-wave rectifier if and only if the difference between the incoming carrier-frequency and the local carrier-frequency is less than the video-filter bandpass. A monitor (Monitor 1) placed at this point can therefore be used to adjust the variable frequency clock to the proper frequency range. It will later be found convenient to adjust the frequency so that the local frequency is less than the incoming frequency.

Search speed is no longer limited by the requirement that carrier frequencies be similar since this requirement is being accomplished separately. An external oscillator can now be used to clock the local sequence-generator so that the sequences drift rapidly by each other. When sequence synchronism is swept through, Monitor 2 observes the discriminator error curve. This curve may be used as a signal to reconnect the sequence-generator-clock bus to the variable frequency clock thus close

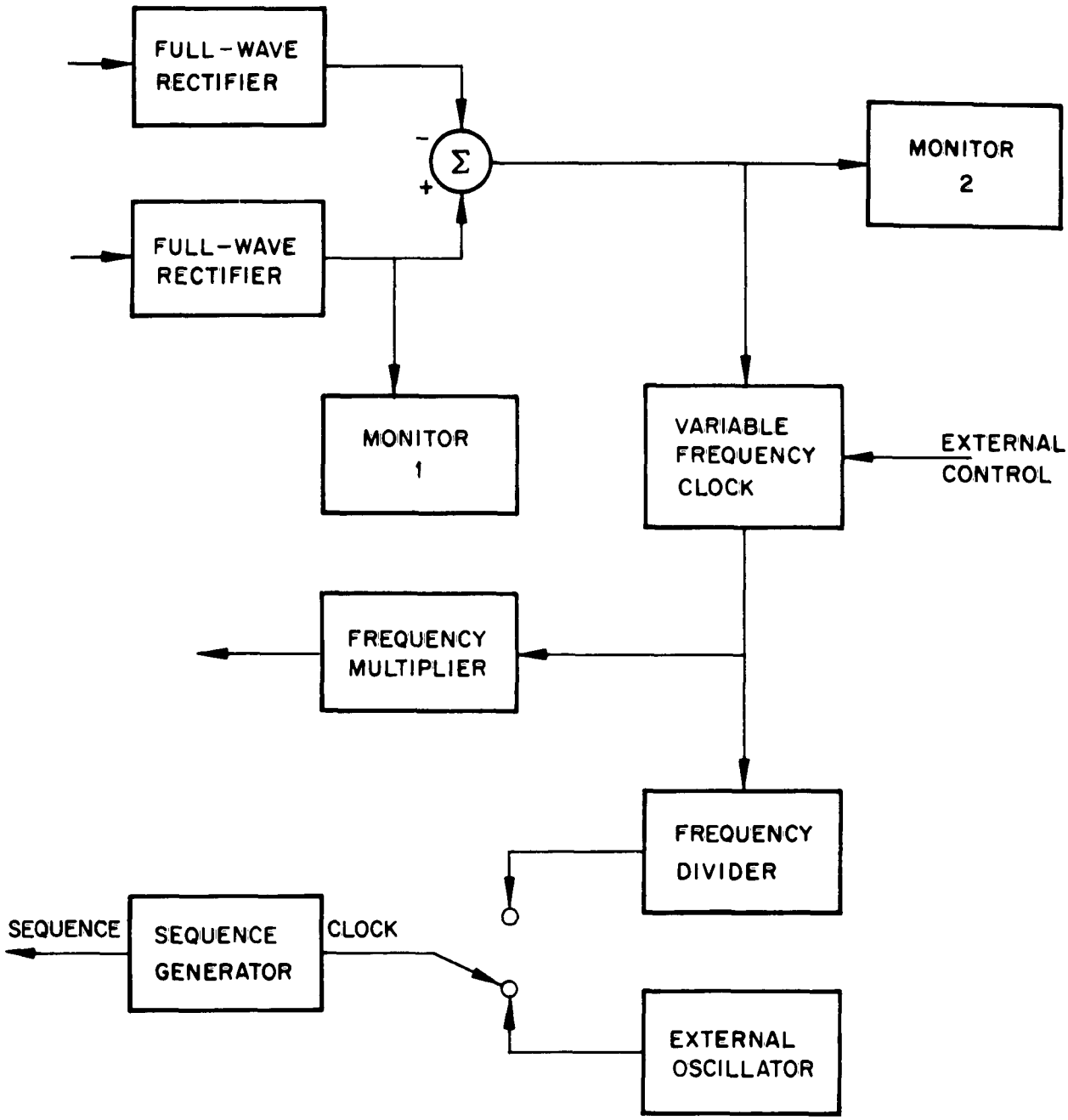

Fig. 2-4 Lock-On Circuitry

the delay-lock loop. Since the local clock-frequency is set below the incoming clock-frequency, the local sequence drifts slowly back into synchronism with the incoming sequence and then it locks in.

Section 3

CHARACTERISTICS OF A TYPICAL DEEP-SPACE COMMUNICATION SYSTEM

3.1 TRACKING

An accurate determination of both the position and the velocity of a spacecraft is needed to assess the progress of a mission, to determine the parameters of midcourse or reentry maneuvers, and to accomplish scientific purposes. Early flights relied on one-way doppler data from the vehicle for radial velocity and angle-of-arrival measurements to give bearing. The Mariner vehicles include a synchronous transponder so that two-way doppler data are obtained which give a radial-velocity measurement accuracy of 0.2 m/sec (Ref. 5). Angular tracking accuracy of ±2 mils with 0.2 to 1.0 mil jitter has been reported using 85-ft diameter receiving antennas (Ref. 6).

Although the radial velocity measurements are quite accurate at present, integration over long periods of time still results in sizeable range errors. Since constant contact with the spacecraft over long periods of time is also necessary, the inclusion of a range-measuring capability is desirable. Improvement of the angular accuracy by more than one order-of-magnitude also appears to be useful. The estimated allowable errors for an improved tracking system are as follows:

Measurement	Allowable Error
Range	±10 meters or 1 part in 10^6, whichever is larger
Range rate	1 part in 10^6
Bearing	0.1 mil absolute, 0.05 mil rms jitter

3.2 COMMAND

Because the commands are neither numerous nor frequent, a very low transmitted bit rate is possible. A rate of 1 bit per second or more, with a bit-error probability of 10^{-5}, is considered satisfactory.

3.3 DATA TRANSMISSION

It is desirable to transmit data at as high a rate as possible for a given error rate. While this transmission speed is greatly dependent on the spacecraft transmitter power and antenna gain, the types of modulation and detection are also important.

It is assumed that data words, each consisting of 5 data bits, are to be transmitted with a word-error probability $\cong 10^{-2}$ and with a corresponding bit-error probability $\cong 2 \times 10^{-3}$.

Section 4

INTEGRATED DELAY-LOCK TRACKING-AND-COMMUNICATIONS SYSTEM FOR A TYPICAL MISSION

4.1 MISSION PARAMETERS

The mission assumed for the following example is a Mars-Venus probe of the Voyager type. Such a space probe might occur in the late 1960's and have the specifications described below.

- Maximum range of operation = 2×10^{11} m (124,000,000 mi) = R_{max}
- Maximum range rate = 10,000 m/sec = $\dot{R}_{max}$
- Maximum acceleration = 10 m/sec^2 = $\ddot{R}_{max}$
- Earth antenna diameter = 210 ft
- Earth antenna gain = 61 db = $G_{T1} = G_{R2}$
- Frequency, earth-spacecraft = 2,113 Mc, λ_1 = 0.142 m
- Frequency, spacecraft-earth = 2,295 Mc, λ_2 = 0.131 m
- Earth transmitter power = 100 kw, CW = P_{T1}
- Spacecraft transmitter power = 25 w, CW = P_{T2}
- Spacecraft antenna diameter = 10 ft
- Spacecraft antenna gain = 34 db = G_{T2}
- Spacecraft command-antenna gain = 3 db = G_{R1}
- Earth-receiver effective noise temperature = 40°K = T_2
- Spacecraft receiver effective noise temperature = 870°K = T_1

Other symbols are defined as follows:

k = Boltzmann's constant

B_{RF} = RF bandwidth

It is assumed that under normal operation the spacecraft high-gain antenna is used both to receive and to transmit. In the event of a loss of attitude control or during a

maneuver, the command antenna may be used to receive. In this case, the required error probability must not be exceeded, although the degradation of other factors such as rapid acquisition can be tolerated.

To determine what configuration of the delay-lock to employ, it is fortunate that the required command-data rate is low. This permits the use of simple envelope detection at the spacecraft because, in spite of a worsening of the SNR, the narrow bandwidth of the spacecraft delay-lock loop results in a low error probability for the command data. Figures 4-1 through 4-5 are block diagrams of the integrated delay-lock tracking-communications system.

4.2 TRANSMITTER

The earth transmitter (Fig. 4-1) contains a stable clock whose frequency is divided to time a 20-stage binary sequence generator. This generator produces a sequence of 1,048,575 digits with a 1.328-Mc clock rate. Each stage of the sequence generator has both direct and complemented outputs available. (In Fig. 4-1, the symbol (19) designates the direct output of the 19th stage, and the symbol $(\overline{19})$ designates the complemented output.) Biphase modulation of the sequence with the command data is accomplished by switching between the direct and complemented output. The sequence is considered to begin when all stages of the shift register contain 1's. At this time, an AND gate enables the command-data bit to begin modulation of the sequence. The condition of the shift register at 150,000 digits later is used to terminate the command modulation by the use of another 20-input AND gate connected to the appropriate direct or complemented generator taps. For the other 898,575 digits, the sequence is transmitted unmodulated. One command-data bit is transmitted for each complete sequence. The biphase-modulated sequence then on-off modulates an RF carrier at 2,113 Mc to produce the transmitted signal.

The reason that only a part of the time is used for command-data transmission is that biphase sequence modulation tends to reduce the delay-lock discriminator output for the simple amplitude system. Command modulation for only a portion of the time

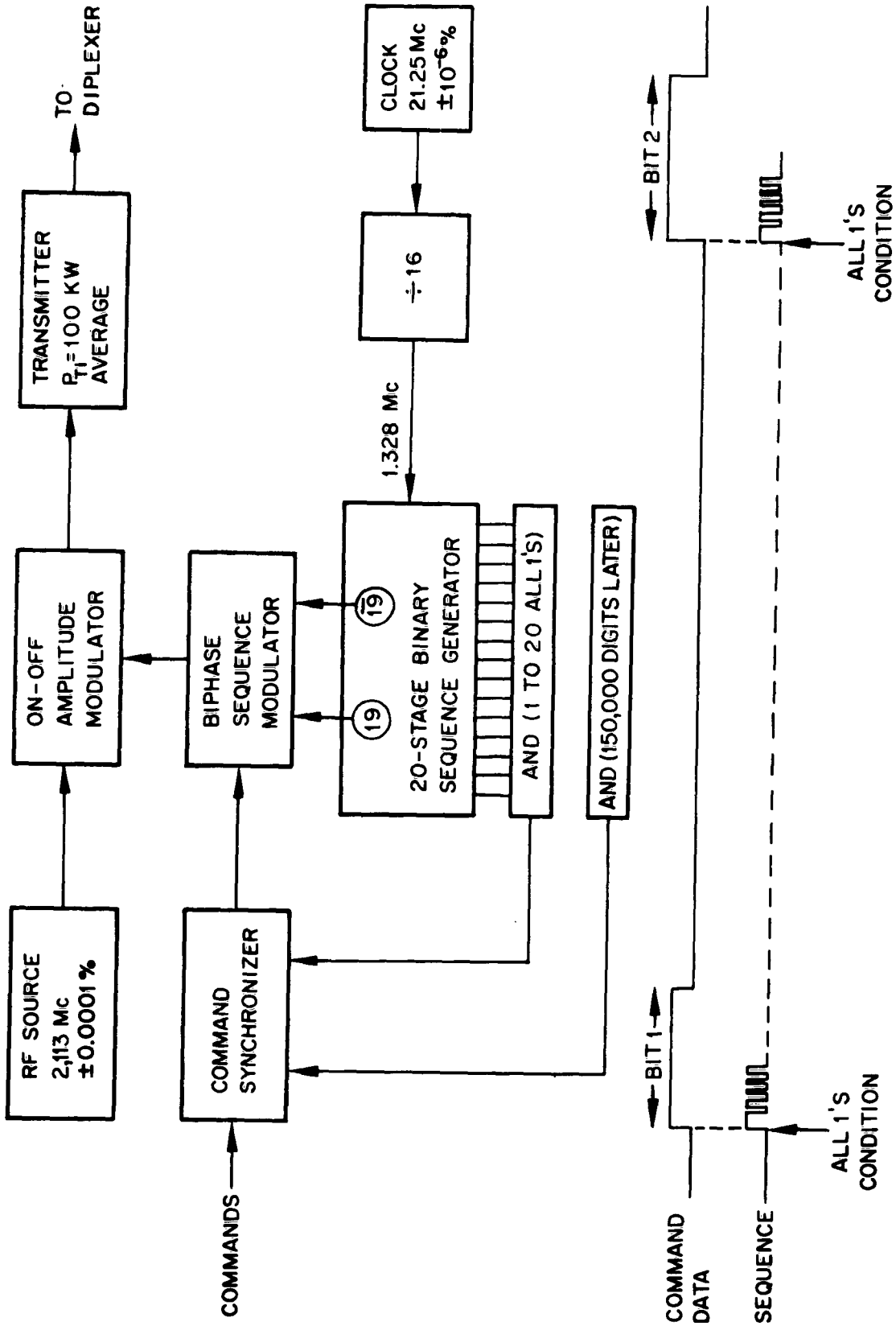

Fig. 4-1 Earth Transmitter

reduces the discriminator output only by that fraction of the time it is present. For the values chosen at this point, the discriminator output is 85.7 percent of its unmodulated output.

4.3 TRANSPONDER

In the spacecraft, there is a transponder (Fig. 4-2) which receives the amplitude-modulated signal, delay-lock tracks the incoming sequence, and demodulates the command data. The transponder also uses the clock and the local sequence generator to produce synchronous transmission of a carrier, the sequence, and data modulation. The operation of the transponder is described in the following paragraphs.

The incoming signal is converted to a 60-Mc intermediate frequency (IF) and the amplitude is detected. The video sequence is then delay-lock tracked as described in subsection 1.2. Command data are removed when the input sequence is correlated with the $n - 1$ tap and then integrated. AND gates identical to those on the earth transmitter are used to dump the integrator at the beginning of the command-bit period and sample the integrator at the end of the period.

The clock frequency is multiplied by 108 to produce a 2,295-Mc synchronous carrier. The direct and complemented outputs of the next-to-the-last sequence-generator stage are switched by the return data to result in a biphase modulation of the sequence.

Data synchronization is based on the output of the 20-input AND gate. When the sequence generator contains all 1's, an output pulse is delivered both to the data synchronizer for frame synchronization and to the 205-bit and 5-bit counters to reset the counters to zero. The 205-bit counter is driven by the 1.328-Mc clock pulses and produces an output for data-bit synchronization each 205 sequence digits. The 205-bit counter output is also counted by a 5-bit counter which produces an output for word synchronization every 5 data bits. It should be noted that the sequence length (1,048,575) factors into $3 \times 5 \times 5 \times 11 \times 31 \times 41 = (205) \times (5) \times 1,023$ so that there

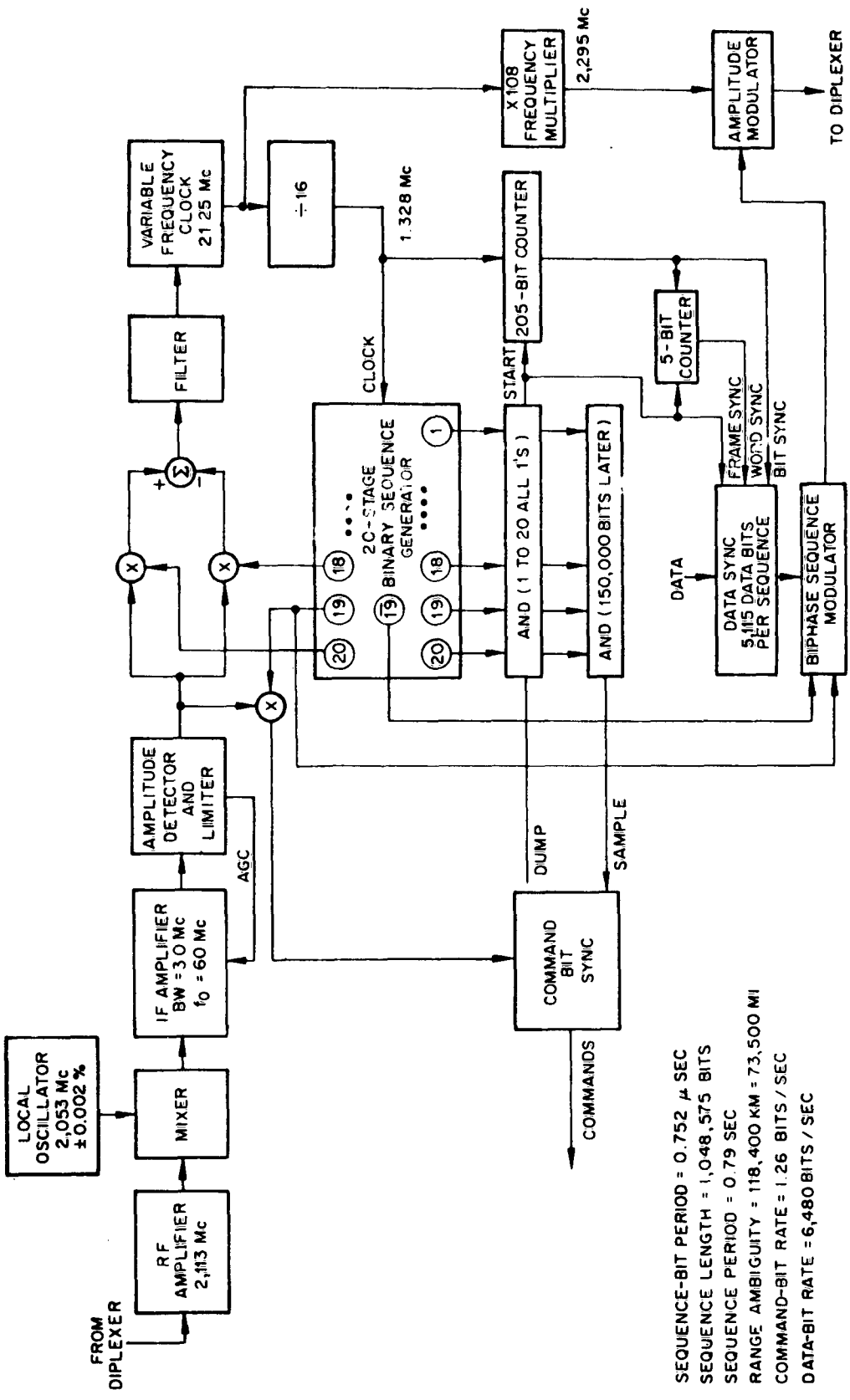

Fig. 4-2 Spacecraft Transponder

are exactly 1,023 words in each sequence and all data bits and words are synchronized with the all-1's condition of the sequence generator.

4.4 TRACKING RECEIVER

When the returned signal is received at the earth, the signal is tracked by a synchronous delay-lock receiver (Fig. 4-3) so that there is no worsening of the SNR. If the receiver is in lock, the clock frequency multiplied by 105 results in a local-oscillator signal nominally at 2,231.25 Mc which is related to the input carrier by the ratio of 105 to 108. The result of mixing the local oscillator and the incoming signal is a nominal 63.75-Mc sequence-modulated IF signal. The clock frequency multiplied by 3 and amplitude modulated by the n and n-2 taps of the sequence generator give synchronous signals for correlation with the input signal to the delay-lock loop. The amplifiers and low-pass filters with bandwidths of 20 kc allow the data modulation to reach the full-wave rectifiers. In the rectifiers, the modulation is removed and only the average value remains to provide error voltage for the delay-lock loop. No nonlinear operations take place until the bandwidth has been narrowed essentially to the bandwidth required by the data. Since the SNR in the data bandwidth is greater than 1, the full-wave pulse rectifier does not significantly change the SNR. Additional filtering after the differencing element then narrows the bandwidth to the tracking bandwidth.

4.5 DATA DEMODULATION

Data are obtained from the incoming signal (Fig. 4-4) by correlation against the n-1 sequence-generator tap. Because the delay-lock loop basically tracks the modulation and not the carrier, the phase of the 63.75-Mc reference carrier is not well controlled with respect to the incoming-carrier phase. To ensure that the phases are never such that the data modulation is lost, a dual correlation is performed by using the reference carrier and a 90-deg shifted reference carrier. Therefore, at least one correlator always produces an output. The video binary sequence appears at the correlator outputs and may be either zero and plus or zero and minus, depending on the relative

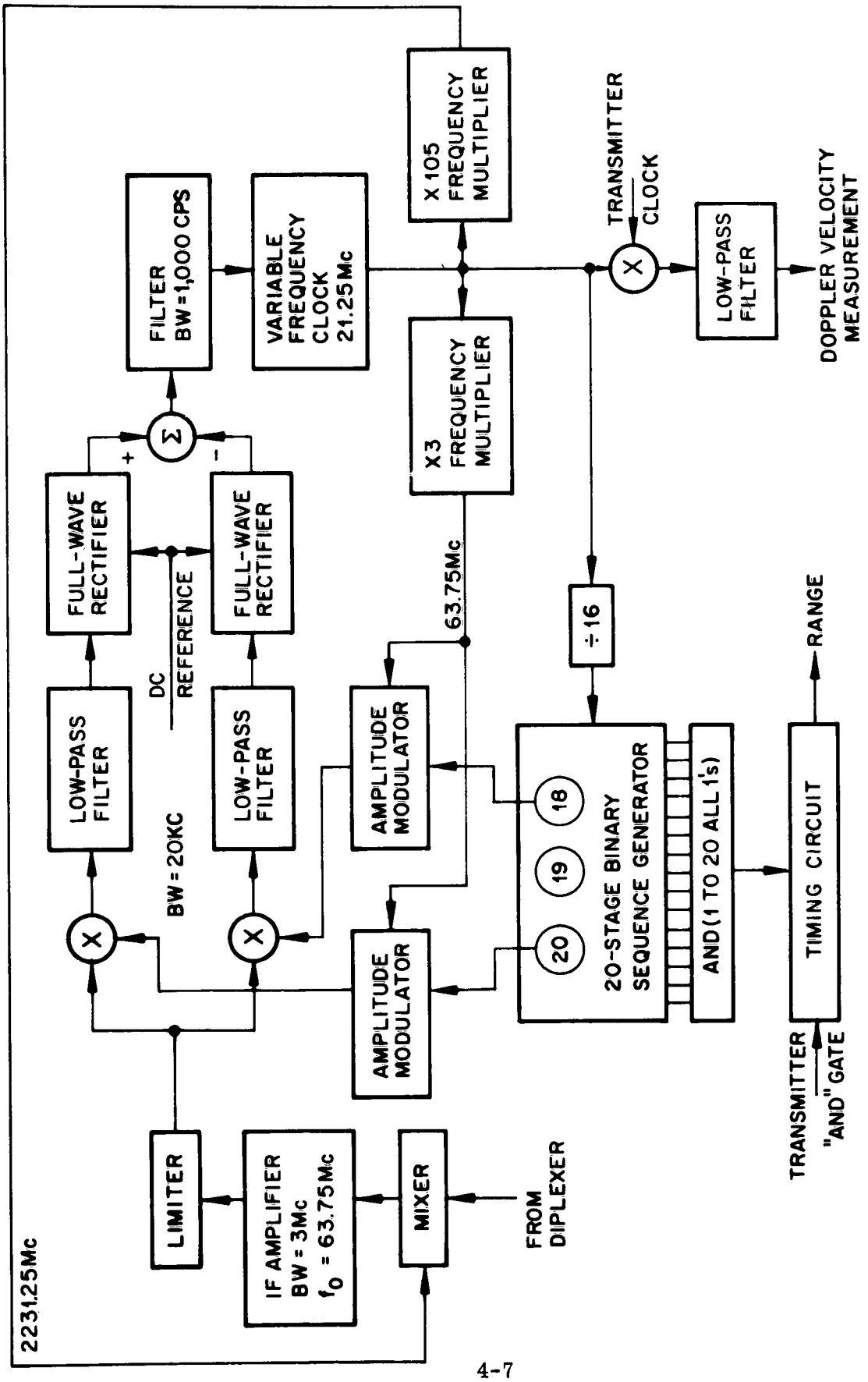

Fig. 4-3 Main Earth-Station Tracking Receiver

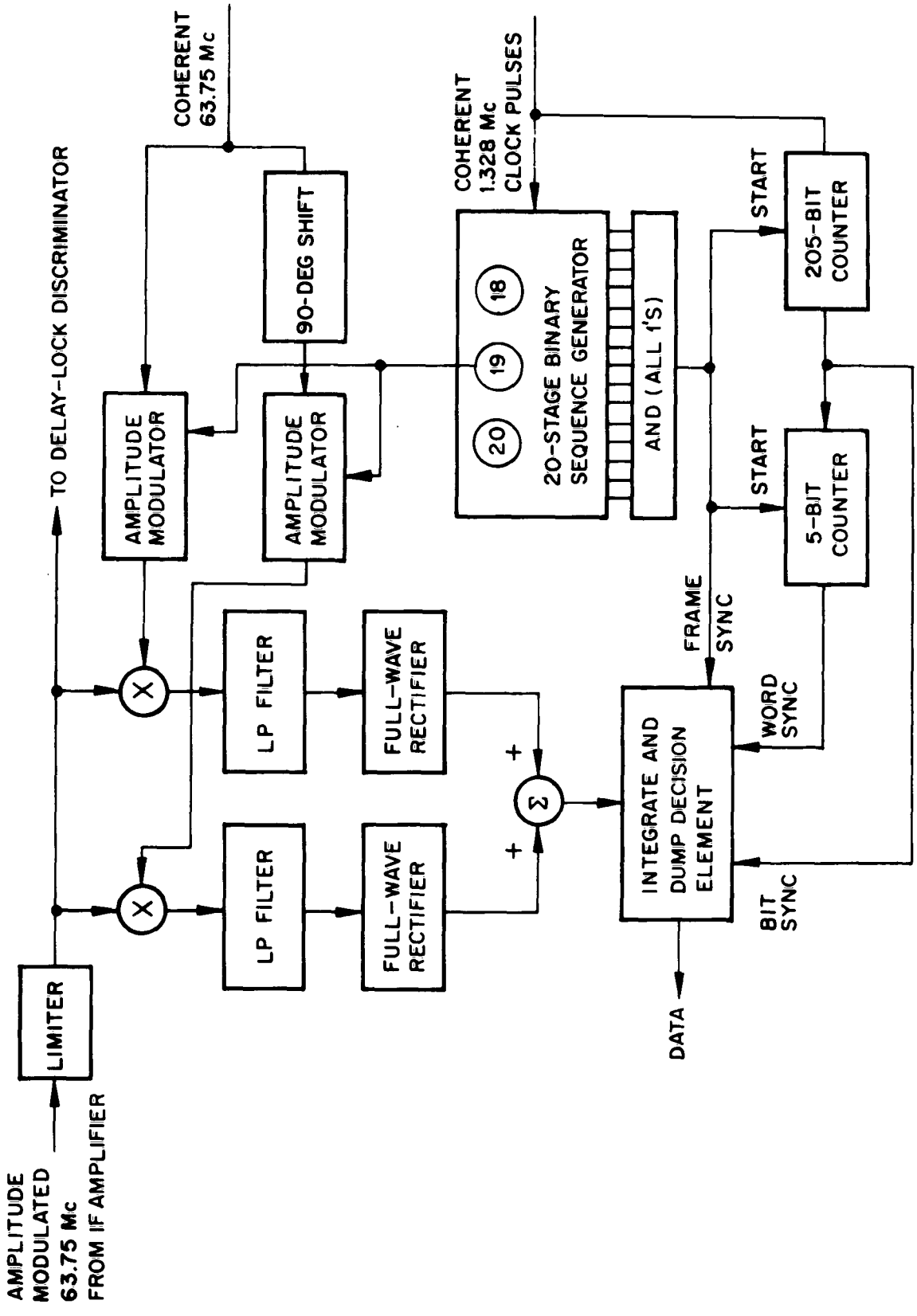

Fig. 4-4 Earth-Station Data Demodulation

carrier phases. In addition, the sequence either may be zero or may be the amplitude of the input envelope, depending on whether a zero or one data bit is being transmitted. The SNR at this point may be very small but, since the detection (correlation) process is linear, no worsening of the SNR occurs.

After the video signals are filtered to remove the sequence and have left only the data zeros (zero voltage) or data ones (nonzero voltage), the results are full-wave rectified and added so that the result is both positive and independent of the relative-carrier phase.* The nonlinear operation occurs after the bandwidth is narrowed so that the SNR is greater than one and, therefore, there is little degradation.

4.6 RANGE AND RANGE RATE MEASUREMENT

Range measurements are made by measuring the time interval between the occurrence of all 1's in the transmitter and receiver sequence generators. Range rate is obtained by measuring the frequency difference between the transmitter clock and the variable-frequency clock of the receiver. The latter clock contains the two-way doppler shift.

4.7 ANGLE TRACKING

Angle tracking may be accomplished either by the usual simultaneous-lobing single-antenna method or by an interferometer method. The latter method has been chosen for example here since the delay-lock technique offers many unique possibilities for such an application. The numerous problems which arise in attempts to achieve a highly accurate interferometer are discussed at length in Appendix A.

The system being considered is shown in simplified form in Fig. 4-5. This system is based on measuring the time-of-arrival differences of the transponded signal at the main station and at two other antennas located 5,000 m from the main station.

---

*The ideal process is to square and then add the two signals, but full-wave rectification gives a similar result with a simpler implementation.

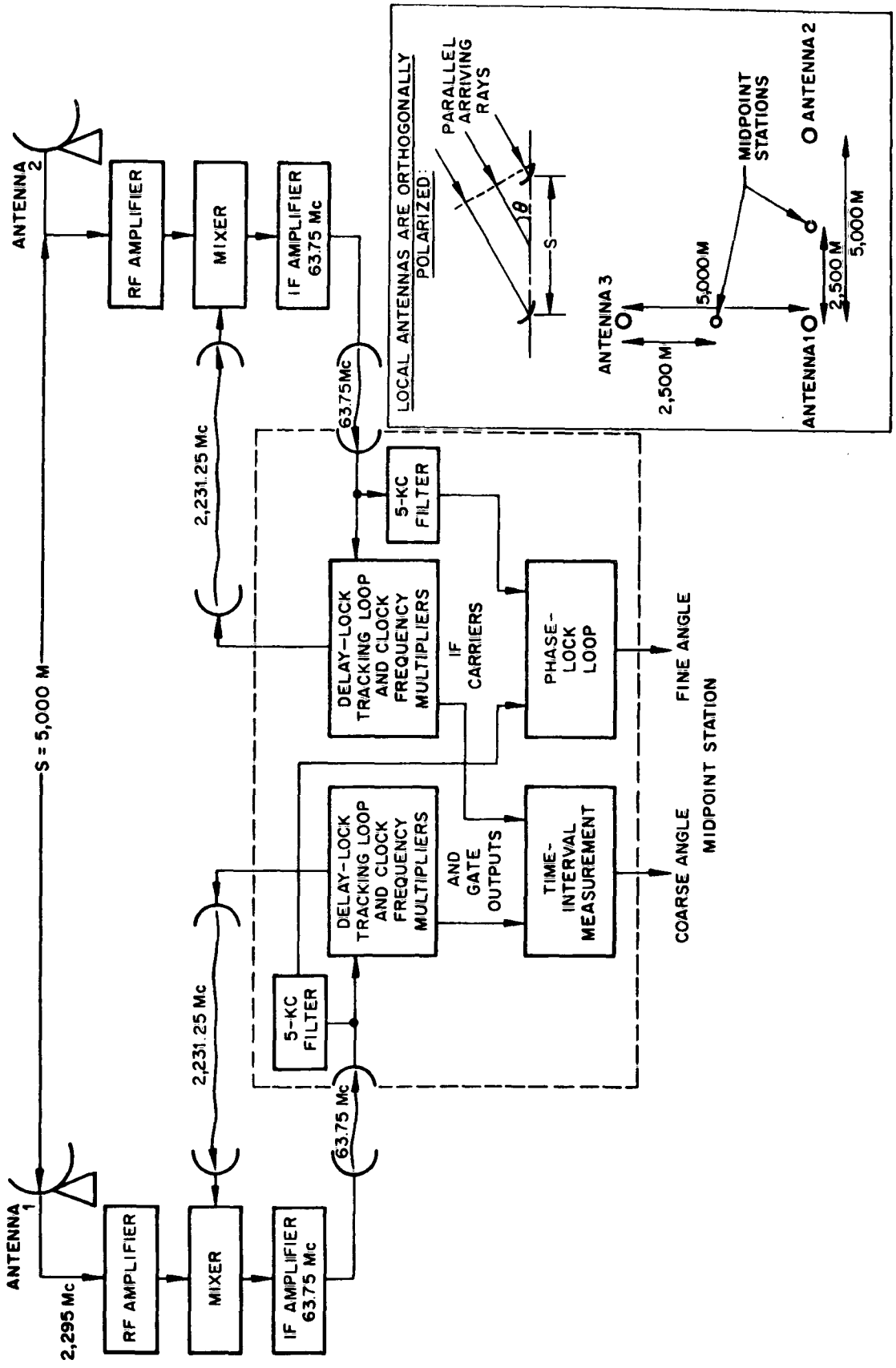

Fig. 4-5 Angle Tracking Portion of Earth Station, One Axis

Stations located at the midpoint of each baseline obtain by relay the received signals in IF form from the antennas. Each signal is delay-lock tracked and coarse-angle data are obtained from measurements of the time interval between similar states of the sequence generators. Fine-angle data are obtained from comparisons of the 63.75-Mc IF-carrier phases by means of a phase-lock loop.

Section 5
EXPECTED PERFORMANCE

5.1 COMMAND DATA

The command error probability is examined on the basis of the low-gain command antenna. The SNR at the input to the transponder amplitude detector is

$$SNR_d = \frac{P_R}{kT_1B_{RF}} = \frac{P_{T1}G_{T1}G_{R1}\lambda_1^2}{kT_1B_{RF}16\pi^2R_{max}^2} \tag{5.1}$$

where P_R is the signal power received by the spacecraft command antenna. Use of the assumed values gives a SNR of 0.0223 in the 3-Mc RF bandwidth. Square-law detection of white, gaussian, independent noise produces a triangular noise spectrum at the detector output. However, for simplicity, the assumption may be made that the detector output spectrum is white and has a value equal to its value at zero frequency. The actual results should be better by a factor of 1.5 to 2.0. With this assumption, the SNR at the command demodulator input is $SNR_i = 0.001$.

The command demodulator uses correlation followed by a synchronized integrate-and-dump decision process. This has been discussed by Harman (Ref. 8) for white, independent, gaussian noise. The important parameters for evaluating the bit-error probability are

$$\bar{u} \triangleq \frac{2E}{N_o} \tag{5.2}$$

where

E = signal energy

N_o = single-sided-frequency power spectral density

Use of the same assumptions regarding the noise and the substitution of $E = P_S\delta$ and $N_o = P_N/B_{LF}$ (where P_S is average signal power, δ is integration time, P_N is average noise power, and B_{LF} is single-sided bandwidth) give

$$\bar{u} = 2B_{LF}\delta(SNR_i) \tag{5.3}$$

where

$$\begin{aligned} B_{LF} &= 1.5 \text{ Mc} \\ \delta &= 0.113 \text{ sec} \\ SNR_i &= 0.001 \\ \bar{u} &= 340 \end{aligned}$$

The decision threshold is placed at $\bar{u}/2$ since an error in predicting the signal present when it is not present is as undesirable as predicting the signal not present when it is present. The error probability is then

$$P\left(\left|\frac{y}{\sigma_y}\right| \geq \frac{\bar{u}}{2\sqrt{(u^2)}}\right) = P\left(\left|\frac{y}{\sigma_y}\right| \geq 9.2\right)$$

For practical purposes, this probability may be considered zero. It is certainly less than the 10^{-5} value specified. When the high-gain antenna is used, the error rate is even lower.

5.2 TRANSPONDER TRACKING AND LOCK-ON

The command-error analysis described previously assumes that the delay-lock loop is continuously in lock and is tracking well. The loop-filter constant (p_o) that is selected must be small enough so that, at maximum range, the SNR in the tracking bandwidth is above the threshold at which tracking performance shows a marked change. Spilker (Ref. 3) chose the threshold condition for the delay-lock loop to correspond to

an SNR such that the rms delay errors equaled 0.30Δ. Theoretical derivations then gave the result

$$\left.\frac{P_S}{p_o N_o}\right|_{Th} = 23.5$$

Later experimental work indicates this value should be

$$\left.\frac{P_S}{p_o N_o}\right|_{Th} = 11.1 \tag{5.4}$$

It is assumed that the latter value can be taken.

A conflicting requirement which arises in setting p_o is that of acquisition, where p_o must be made large enough for rapid acquisition. Spilker also analyzes this problem and shows that in order to provide lock-on under strong signal conditions the normalized search velocity $\dot{y}$ must be

$$|\dot{y}|_{max} \leq 2.2$$

$$\dot{y} \triangleq \frac{1}{p_o \Delta}\frac{dT}{dt} \tag{5.5}$$

where

Δ = digit duration ($0.752\ \mu$sec)

$\frac{dT}{dt}$ = rate of search of delay time

When the search is linear,

$$\frac{dT}{dt} = \frac{T_S}{T_{a,\,max}} \tag{5.6}$$

where

T_S = duration of the sequence

$T_{a,\,max}$ = maximum acquisition time (the time required to search the complete sequence)

Then,

$$T_{a,\,max} = \frac{T_S}{|\dot{y}|_{max}\, p_o\, \Delta} \tag{5.7}$$

A third requirement on p_o is that it must be large enough to maintain lock-on during the largest delay accelerations which are encountered. For the delay-lock filter considered by Spilker, the closed-loop transfer function of the delay-lock loop is

$$\frac{\hat{T}}{T} = \frac{1 + \sqrt{2}\; p/p_o}{1 + \sqrt{2}\; p/p_o + (p/p_o)^2} \tag{5.8}$$

The tracking error is

$$(T - \hat{T}) = T\left[\frac{(p/p_o)^2}{1 + \sqrt{2}\; p/p_o + (p/p_o)^2}\right] \tag{5.9}$$

If the delay input has a constant acceleration $T = 1/2\, a_d t^2$, then $T(p) = a_d/p^3$. The steady-state delay error is

$$\epsilon_{SS} = \lim_{p \to o} pT(p)\left[\frac{(p/p_o)^2}{1 + \sqrt{2}\; p/p_o + (p/p_o)^2}\right] = \frac{a_d}{p_o^2} \tag{5.10}$$

The delay acceleration (a_d) is related to the space acceleration (a) by

$$a = c\, a_d \tag{5.11}$$

where c = velocity of propagation. If it is assumed that the steady-state error should be kept less than $\Delta/3$, the requirement on the tracking loop bandwidth is

$$p_o \geq \sqrt{\frac{3a}{\Delta c}} \tag{5.12}$$

For the two values $a = 10\ m/sec^2$ and $\Delta = 0.752\ \mu sec$, the tracking-loop bandwidth must be greater than 0.364 rad/sec. This is no limitation, since all other criteria point to a larger bandwidth than this.

When the threshold condition is considered, use is made of the fact that the delay-lock loop improves the SNR by the ratio of input bandwidth to closed-loop bandwidth. That is,

$$\frac{SNR_o}{SNR_i} = \frac{B_{LF}}{B_n} = \frac{B_{LF}}{0.53\ p_o} \tag{5.13}$$

If the output SNR is set equal to the threshold value of 11.1, the maximum tracking-loop bandwidth is obtained

$$p_o \leq \frac{B_{LF} SNR_i}{0.53\ SNR_{Th}} = 0.17\ B_{LF}\ SNR_i \tag{5.14}$$

Only the energy in the sidebands is effective for tracking, so SNR_i refers to the SNR with the carrier deleted. When the command antenna is used, the result is $p_o \leq 127$ rad/sec ; when the high-gain antenna is used, the result is $p_o \leq 1.59 \times 10^5$ rad/sec. The corresponding values of maximum-acquisition time are $T_{a,\,max} = 3,740$ sec (62.4 min) with the command antenna and $T_{a,\,max} = 3.0$ sec with the high-gain antenna. The latter is not a realistic choice because the signal must make the complete round trip, a time of some 20 min at maximum range. The choice suggested here is to use two tracking-loop bandwidths and search velocities in the transponder switched by receiver AGC. When the AGC voltage is low, the loop bandwidth is 127 rad/sec; when the voltage is high, the loop bandwidth is 2,500 rad/sec. The maximum acquisition time of the transponder is therefore 3 min, 10 sec during most of the flight and is possibly 62.4 min under conditions of maneuver or malfunction. During most

of the flight, the transponder delay-lock loop operates more than 20 db above threshold and there is the possibility of operation at threshold in the case of maneuver or malfunction at maximum range.

When the command antenna is used, the long transponder lock-on time is not a fundamental limitation. Sequence-length switching can be employed to allow the use of a short sequence for acquisition. Then, when lock-on has been achieved, a command can switch operation to the long sequence.

5.3 EARTH-STATION TRACKING AND LOCK-ON

Primes are used to indicate quantities for the earth receiver, when it is necessary to distinguish from the same symbols used in the transponder. The SNR at the delay-lock input is

$$SNR_i' = \frac{P_{T2}\, G_{T2}\, G_{R2}\, \lambda_2^2}{kT_2\, B_{RF}\, 16\, \pi^2\, R_{max}^2} \tag{5.15}$$

$$SNR_i' = 0.13$$

The delay-lock tracking bandwidth must be at least 17.5 kc to pass the data modulation to the full-wave rectifier and thus provide tracking error. If it is 20 kc, the SNR input to the pulse rectifier is

$$SNR_p = SNR_i' \frac{B_{LF}}{B_F} = 19.5$$

This shows $SNR_p > 1$ so that the pulse rectifiers do not much worsen the SNR.

The bandwidth does not have to be narrowed any to achieve threshold SNR; however, the bandwidth may be narrowed considerably without an excessively increased

acquisition time. An overall tracking-loop bandwidth of 6,280 rad/sec results in

$$T'_{a,\max} = \frac{T_S}{|\dot{y}|_{\max} p'_0 \Delta} = 76 \text{ sec}$$

5.4 RANGE ACCURACY AND AMBIGUITY

The binary sequence generator has 20 stages. With the 1.328-Mc clock, this choice results in a sequence period of 0.79 sec and a corresponding range ambiguity of 73,500 mi. A longer generator would result a longer unambiguous range, but it would also increase the acquisition time and add to equipment complexity. The proper sequence to use in a synchronous system also depends on the factors of the sequence length. These factors are given in Table 5-1 for a number of possible sequence lengths.

Table 5-1

FACTORS OF SEQUENCE LENGTH FOR A SYNCHRONOUS SYSTEM

Number of Sequence Generator Stages	Sequence Length	Factors of Sequence Length
15	32,767	$7 \times 31 \times 151$
16	65,535	$3 \times 5 \times 17 \times 257$
17	131,071	Prime
18	262,143	$3 \times 3 \times 3 \times 7 \times 19 \times 73$
19	524,287	Prime
20	1,048,575	$3 \times 5 \times 5 \times 11 \times 31 \times 41$
21	2,097,151	$7 \times 7 \times 127 \times 337$
22	4,194,303	$3 \times 23 \times 89 \times 683$
23	8,388,607	$47 \times 178,481$
24	16,777,215	$3 \times 3 \times 5 \times 7 \times 13 \times 17 \times 241$
25	33,554,431	$61 \times 601 \times 1,801$

Several of the lengths shown in Table 5-1 are not suitable either because they are prime or because the factors do not result in appropriate data-bit or data-word lengths.

The 20-stage generator fits these requirements and is a compromise between range ambiguity and acquisition time. In tracking a space vehicle, the velocity and position history since launch is always well known, so an ambiguity of 73,500 mi should be no handicap.

5.5 RANGE ERROR

Except at close range, the range error is dependent primarily on errors in knowledge of the propagation velocity. The total delay time at maximum range is approximately 1,333 sec and, since the propagation velocity is known to about 10^{-6}, the equivalent time error is 1,333 μsec. For long sequences, the variance of the time-delay measurement (Ref. 3) due to noise is

$$\sigma_T^2 = 2.12\Delta^2 \frac{N_o p_o}{P_S} \tag{5.16}$$

When the command antenna is used, the maximum-range SNR in the transponder is $SNR_{Th} = 11.1$ which gives $\sigma_T = 0.33$ μsec; this error is much less than the propagation-velocity error. The term P_S is inversely proportional to the square of the range so that σ_T, like the propagation error, is directly proportional to the range. At shorter ranges, practical equipment problems are the limitations. Experience has indicated that for strong signals the tracking error can be held to about $\Delta/100$; this is 7.52 nsec, which corresponds to a range error of 1.12 m.

5.6 RANGE RATE ERROR

The range rate is calculated from

$$\dot{R} = \frac{f_d}{f_c} \frac{c}{2} \tag{5.17}$$

where

f_d = measured difference frequency

f_c = clock frequency

The stability of the main earth-station clock is a factor in the error. However, it is no great problem to obtain stability of 10^{-9} - 10^{-10} in the oscillator. The accuracy is really limited by the accuracy with which c is known. Thus, the range-rate error is within $\pm 10^{-6}$.

5.7 ANGLE TRACKING ERROR

Angle accuracy is determined by many factors, including the accuracy with which the time-of-arrival delay at two antennas can be measured. Other factors which determine angle accuracy are listed below.

- Spacing of the antennas
- Accuracy and stability of antenna spacing
- Accuracy of propagation velocity in the neighborhood of the antennas
- Propagation velocity anomalies in the atmosphere
- Refractive bending in the atmosphere

These factors are discussed at some length in Appendix A. The conclusion reached is that it should be possible, with some difficulty, to maintain at less than 0.05 mil the angular error caused by these factors.

The relation between delay error σ_T and angular error σ_θ is

$$\sigma_\theta = \frac{c}{S \sin \theta} \sigma_T \tag{5.18}$$

where

c = velocity of propagation

θ = angle-of-arrival with reference to the horizontal (see Fig. 4-5)

If accurate tracking is required for $\theta \geq 20$ deg, antenna spacing of 5,000 m and $\sigma_\theta = 0.05$ mil give as the required delay error $\sigma_T = 0.285$ nsec.

Phase measurements in a phase-lock loop may be made with an accuracy of about 3 deg. For a 63.25-Mc carrier, 3 deg corresponds to 0.132 nsec so that the required accuracy is possible.

It is necessary to set the delay-lock-loop bandwidth so that the mean-square error in coarse-time measurement is less than the ambiguity of the fine-time measurement; that is,

$$\sigma_{Td\ell} \leq \frac{1}{f_{IF}} = 15.8 \text{ nsec}$$

The use of

$$\sigma^2_{Td\ell} = 2.12\Delta^2 \frac{N_o p_o}{P_S} \tag{5.19}$$

gives the required delay-lock filter constant p_o to be 1,030 rad/sec. Although this is less than the search bandwidth, it is possible after lock-on to reduce the bandwidth to this amount.

5.8 DATA-BIT ERROR PROBABILITY

The data demodulation process is the same as the command demodulation process and, therefore, Eq. (5.2) is applicable. For this case, the SNR in a bandwidth of 1.5 Mc is $SNR_i = 0.065$.

The integration time is $\delta = 205 \times 0.752 \times 10^{-6} = 154 \times 10^{-6}$ sec. The resulting value for $\bar{u}$ is

$$\bar{u} = 30 = \overline{u^2}$$

The bit error probability, then, is

$$P\left(\frac{y}{\sigma_y} \geq \frac{\bar{u}}{2\sqrt{(\bar{u}^2)}}\right) = P\left(\frac{y}{\sigma_y} \geq 2.75\right) \cong 3 \times 10^{-3}$$

5.9 SUMMARY

A summary of expected performance is shown in Table 5-2.

Table 5-2

EXPECTED PERFORMANCE SPECIFICATIONS

Item	Specification
Maximum range	2×10^{11} m
Range ambiguity	1.18×10^{8} m = 73,500 mi
Range error	1.12 m or 1 in 10^6, whichever is larger
Range-rate error	1 in 10^6
Angular error	0.05 mil rms
Acquisition time:	
Directional antenna	4.5 min maximum plus two-way transmission time
Omnidirectional antenna	31.2 min average, 62.4 min maximum
Command-bit error probability	$< 10^{-5}$
Data-bit error probability	$< 3 \times 10^{-3}$
Command rate	1.26 bits/sec
Data rate	6,480 bits/sec

The performance specifications shown in Table 5-2 indicate a very advanced capability. Much of this is due, of course, to the assumption of system factors such as antenna gain and transmitter power, which do not have exclusive connections with

delay-lock tracking. It is not the purpose of this paper to compare various systems, but, rather, to show how delay-lock techniques can be utilized in an integrated deep space tracking-communications task. The system which is described and analyzed does appear to have excellent capability.

Section 6

REFERENCES

1. J. J. Spilker, Jr., and D. T. Magill, "The Delay-Lock Discriminator – An Optimum Tracking Device," Proc. Inst. Radio Engrs., Vol. 49, Sep 1961, pp. 1403–1416

2. M. R. O'Sullivan, "Tracking Systems Employing the Delay-Lock Discriminator," Trans. Inst. Radio Engrs., Vol. SET-8, Mar 1962, pp. 1–7

3. Lockheed Missiles & Space Company, Delay-Lock Tracking of Binary Signals, by J. J. Spilker, Jr., 9-90-62-85, Sunnyvale, Calif., Sep 1962

4. W. G. Weiss and M. Evans, "Application of the Delay-Lock Discriminator to the Satellite Rendezvous Problem" (paper presented at Aerospace and Navigational Electronics Conference, Baltimore, Md., Oct 1962)

5. California Institute of Technology, Jet Propulsion Laboratory, Operational Status of the Deep Space Instrumentation Facility as of 1 July 1962, by J. W. Thatcher, CIT/JPL TR-32-319, Pasadena, Calif., 13 Aug 1962

6. R. P. Mathison, "Tracking Techniques for Interplanetary Spacecraft," Proceedings of the National Telemetering Conference, Washington, D.C., May 1962

7. Encyclopaedic Dictionary of Physics, Vol. 7, New York, Pergamon Press, 1962, p. 611

8. W. W. Harman, Principles of the Statistical Theory of Communications, New York, McGraw-Hill, 1963

9. Lockheed Missiles & Space Company, Threshold Comparison of Phase-Lock, Frequency-Lock, and Maximum Likelihood Types of FM Discriminators, by J. J. Spilker, Jr., 2-43-61-2, Sunnyvale, Calif., Jul 1961

10. V. A. Counter (private communication)

11. Handbook of Geophysics, New York, Macmillan, 1960

12. J. W. Herbstreit and M. C. Thompson, "Measurements of the Phase of Radio Waves Received Over Transmission Paths With Electrical Lengths Varying as a Result of Atmospheric Turbulence," Proc. Inst. Radio Engrs., Oct 1955, p. 1391

13. D. K. Barton, "Reasons for the Failure of Radio Interferometers to Achieve Their Expected Accuracy," Proc. Inst. Radio Engrs., Apr 1963, p. 626

14. M. C. Thompson, H. B. James, and R. W. Kirkpatrick, "An Analysis of Time Variations in Tropospheric Refractive Index and Apparent Radio Path Length," J. Geophys. Res., Vol. 65, Jan 1960, pp. 193–201

15. A. P. Deam and B. M. Fannin, "Phase Difference Variations in 9350-Mc Radio Signals Arriving at Spaced Antennas," Proc. Inst. Radio Engrs., Oct 1955, p. 1402

16. R. S. Grisetti and E. B. Mullen, "Baseline Guidance Systems," Trans. Inst. Radio Engrs., MILE, Dec 1958, pp. 36–44

17. Space Age Electronics, Vol. 2, Chapter 7, Section 7.4 (book to be published)

18. Radio Corporation of America, Instrumentation Radar AN/FPS-16 (XN-2), by A. J. Mills et al., 869 FR, Moorestown, N.J., 1956

Appendix A

ACCURACY LIMITATIONS ON THE ANGULAR TRACKING OF SPACE VEHICLES AND SATELLITES BY THE USE OF RADIO INTERFEROMETERS

A. 1 INTRODUCTION

Angular tracking of satellites and space vehicles by means of radio has been accomplished by both lobing radars and radio interferometers, and the angular accuracy obtained to date has varied from 0. 5 mil to several mils. In calculating satellite orbits and injection conditions for space vehicles, this amount of error has been a severe limitation.

This appendix investigates the possibility of improving the angle-tracking capability of radio interferometers to result in errors of only 0. 01 to 0. 05 mil. Such an accuracy is suggested by the analysis of a system which uses a combination of delay-lock and phase-lock tracking methods (Ref. 2). This analysis is based only on the basic delay and phase-measuring capabilities of the electronic system. Other principal factors which affect the accuracy are discussed in this appendix. These factors are (1) anomalies of propagation velocity of radio waves through the ionosphere and troposphere, (2) changes of propagation velocity in the region of the interferometer, and (3) changes of baseline length separating the interferometer antennas.

With proper site selection, much care in design, and continuous built-in calibration procedures, radio interferometers which have long baselines are capable of an angular accuracy from 0. 01 to 0. 05 mil rms.

A. 2 REPRESENTATION OF INTERFEROMETERS

Whether operating by phase or delay measurement, the ideal interferometer measures the difference in radio-signal propagation times from a target to each of two antennas having a known separation (Fig. A-1). The angle of the target is then calculated from

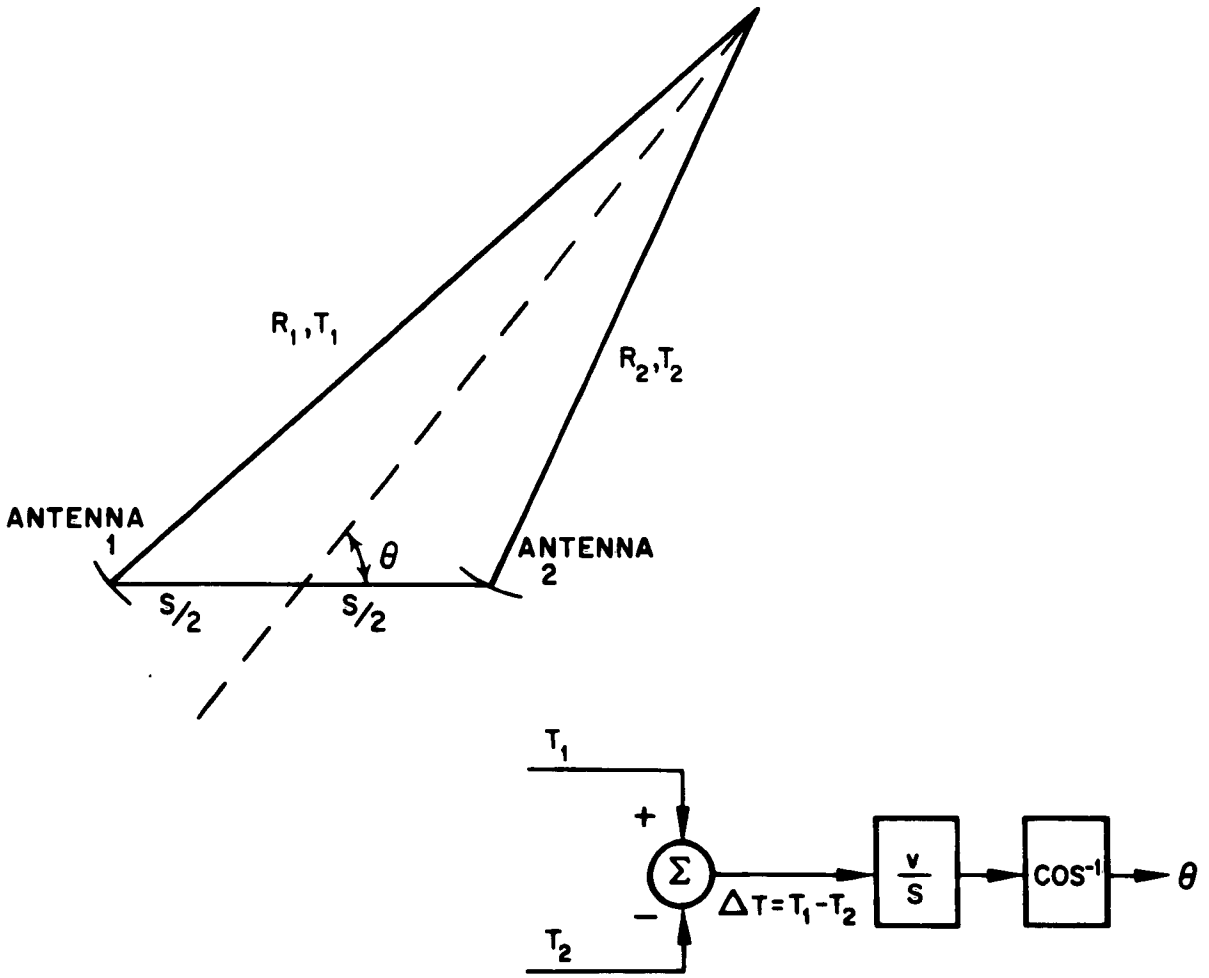

Fig. A-1 Representation of an Interferometer

the time difference of arrival (ΔT), the known separation (S), and the velocity of propagation in the vicinity of the interferometer (v). The target-bearing angle θ is measured from a point at the center of the baseline which joins the antennas. An approximate formula [Eq. (A.1)] gives the angle as

$$\cos \theta_a = \frac{v \Delta T}{S} \qquad \text{(A.1)}$$

where the subscript indicates the approximation. An analysis by Counter (Ref. 10) shows the exact form to be

$$\cos\theta = \frac{v\,\Delta T}{S}\left\{1 - \frac{S^2}{4\bar{R}^2}\left[1 - \left(\frac{v\,\Delta T}{S}\right)^2\right]\right\}^{-1/2} \qquad \text{(A.2)}$$

where

$$\bar{R} \triangleq \frac{R_1 + R_2}{2}$$

If the average range is not large when compared to the antenna separation, the error resulting from use of the approximate form may be excessive. The error caused by use of the approximate form is nearly

$$\delta\theta_a \cong \frac{S^2}{16\bar{R}^2}\sin 2\theta_a \qquad \text{(A.3)}$$

The maximum error for any $\bar{R}/S$ occurs at $\theta_a = 45$ deg. In order to maintain the maximum error less than 0.01 mil, $\bar{R}/S > 80$. For a satellite tracking system, $\bar{R}$ may be as small as 100 mi. The distance between antennas is then limited to 1.25 mi. This is approximately the distance which appears to be desirable from other considerations, so range measurement may or may not be required. In the case of a deep space tracking interferometer, range measurement is not necessary.

A.3 ANALYSIS OF ERRORS

A.3.1 Angular Error Due to Range Error

When Eq. (A.2) is differentiated with respect to range and when suitable approximations are made, the angular error due to range error is

$$\delta\theta_{\bar{R}} \cong -\frac{S^2}{8\bar{R}^2}\sin 2\theta_a \frac{\delta\bar{R}}{\bar{R}} \qquad \text{(A.4)}$$

If $\bar{R}/S > 20$, the fractional range error in order to maintain $\delta\theta_{\bar{R}} < 0.01$ mil is 0.032. Therefore, even a very crude range measurement is satisfactory in those cases where it is needed.

A.3.2 Angular Error Due to Propagation-Velocity Error

Differentiation of Eq. (A.1) with respect to v gives the relation between the angular error and propagation-velocity error as

$$\delta\theta_v \cong - \cot\theta \frac{\delta v}{v} \tag{A.5}$$

It is assumed that precise tracking is required for $\theta \geq 20$ deg . When $\theta = 20$ deg, the maintenance of $\delta\theta_v \leq 10^{-5}$ requires $\frac{\delta v}{v} \leq 0.36 \times 10^{-5}$. Observations of the propagation velocity at the surface (Ref. 11) have given extreme fractional changes in v of $\pm 4 \times 10^{-5}$ with various locations and weather conditions. Reference 12 shows variations in v of $\pm 4 \times 10^{-6}$ in an hour. Therefore, it is necessary to calibrate the site, either by meteorological or by radio means, to determine the proper value for v . For antenna separations less than a few hundred feet, the paths over which v must be averaged are near the surface; consequently, surface observations to determine v are sufficient. For larger separations, v may have to be averaged over paths which include altitudes of several thousand feet. For such cases, radiosonde meteorological data might be required. In extreme cases of antenna separation (S > 10,000 ft), it would probably be necessary to employ a correction for v , which was a function of the indicated angle, to account for the fact that ΔT_v is a path near the surface for $\theta \cong 90$ deg or $\theta \cong 0$ deg and is a path extending to thousands of feet altitude for $\theta \cong 45$ deg .

A.3.3 Angular Error Due to Antenna-Spacing Error

Differentiation of Eq. (A.1) with respect to S gives the angular error due to errors or variations in distances between antennas as

$$\delta\theta_S \cong \cot\theta \frac{\delta S}{S} \tag{A.6}$$

A rather difficult restriction arises from Eq. (A.6). With use of $\theta = 20$ deg, the required fractional error in spacing is seen to be $\frac{\delta S}{S} \leq 0.36 \times 10^{-5}$. For a 100-ft baseline, the phase centers of the two antennas must not vary more than 0.0043 in. This practically rules out movable high-gain antennas except for ones with very long baselines. Short-baseline antennas must either be broad-beamwidth fixed antennas or be mounted on a pivot arm which keeps θ near zero to minimize the errors caused by S and v. The latter configuration is essentially a standard radar-angle-tracking system and requires a measurement of 0.01 mil for the angular position of the arm. This is a delicate mechanical task.

The term S/v in Eq. (A.1) is the propagation time from one antenna to the other. Therefore, continuous calibration of the surface conditions (both S and v) is provided when the capabilitity to measure the round-trip transmission time between antennas is incorporated into the system design. Since the antenna round-trip time may be measured with accuracy greater than 10^{-5}, any uncertainty which remains lies in the variation of v with altitude.

A.3.4 Angular Errors Due to Propagation Anomalies

If the interferometer antennas are separated widely enough, the tropospheric conditions are sufficiently different over the two paths to cause significant errors in ΔT. Differentiation of Eq. (A.1), with respect to ΔT gives

$$\delta \theta_{\Delta T} = - \frac{v}{S \sin \theta} \delta(\Delta T) \qquad (A.7)$$

The error from propagation anomalies is smallest at $\theta = 90$ deg. Since S appears in the denominator, the error apparently could be reduced by an increased separation of the antennas. However, $\delta(\Delta T)$ is zero for small separation, where the ray paths are identical, and increases as the separation increases. This effect may tend to cancel the decrease of angular error due to increased antenna separation.

Barton (Ref. 13) attempts to use certain data obtained by NBS (Ref. 14), to determine the variation of $\delta(\Delta T)$ with antenna spacing S. The NBS data give the variation of measured radio range (equivalent to propagation time) between fixed points on the earth's surface. One set of measurements is from a mountain top to sea level in Hawaii, and another is between two mesas near Boulder, Colorado. These data are supplemented over longer time periods by calculations of a refractive-index variation. The refractive index is based on twice-hourly meteorological data obtained over a period of several years at the Denver airport. The result of the measurements is the estimated spectral density of one-way range variation as shown in Fig. A-2 which is an approximation of the NBS data (Ref. 15). Barton then assumed a model of the troposphere consistent with this spectral density. His model, as shown in Fig. A-3, pictures the troposphere as being a medium having a refractive index which is a random function of position normal to the ray path. This medium drifts through the ray path and causes variations of propagation time along the path. If the average drift velocity is v_w, then the interferometer which obtains the difference of propagation times at two positions acts approximately as a high-pass filter with a cutoff frequency of $f_b = 0.22 \frac{v_w}{S}$. See Fig. A-4. The product of the functions of Figs. A-2 and A-4 is the spectral density of error due to tropospheric anomalies and the product can be integrated to obtain the variance of the error. Barton's results indicate that an antenna separation of about 60,000 ft is needed to maintain the angular error below 0.01 mil.

Other tests which have been performed over relatively short periods of time (Refs. 12 and 15) appear to disagree with Barton's predictions and suggest that antenna separation of only a few thousand feet is necessary. Herbstreit and Thompson (Ref. 12) report the results of relative phase-of-arrival measurements made at separated receiving antennas with a 1,046-Mc signal transmitted from Pike's Peak. When these measurements were obtained, the receiving antennas were located at the Garden of the Gods, 10 mi distant and about 7,000 ft lower in elevation. In a period of an hour, the total RF phase showed a variation of about 70 deg over each of the paths; however, the phase differences were 8 deg for 500-ft receiving-antenna separation, 18 deg for 1,420-ft separation, and 19 deg for 1,920-ft separation. When translated into

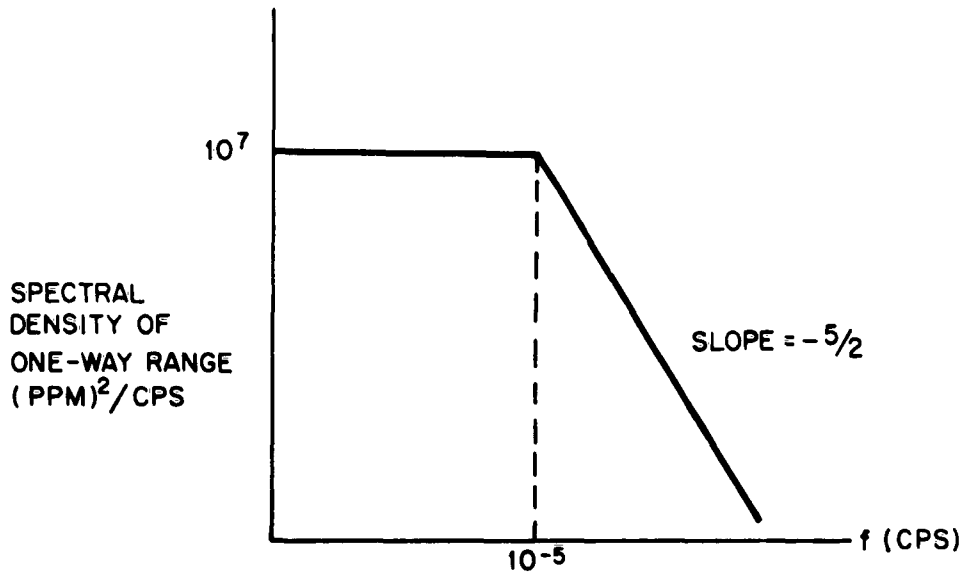

Fig. A-2 Spectral Density of One-Way Variation in Radio Range

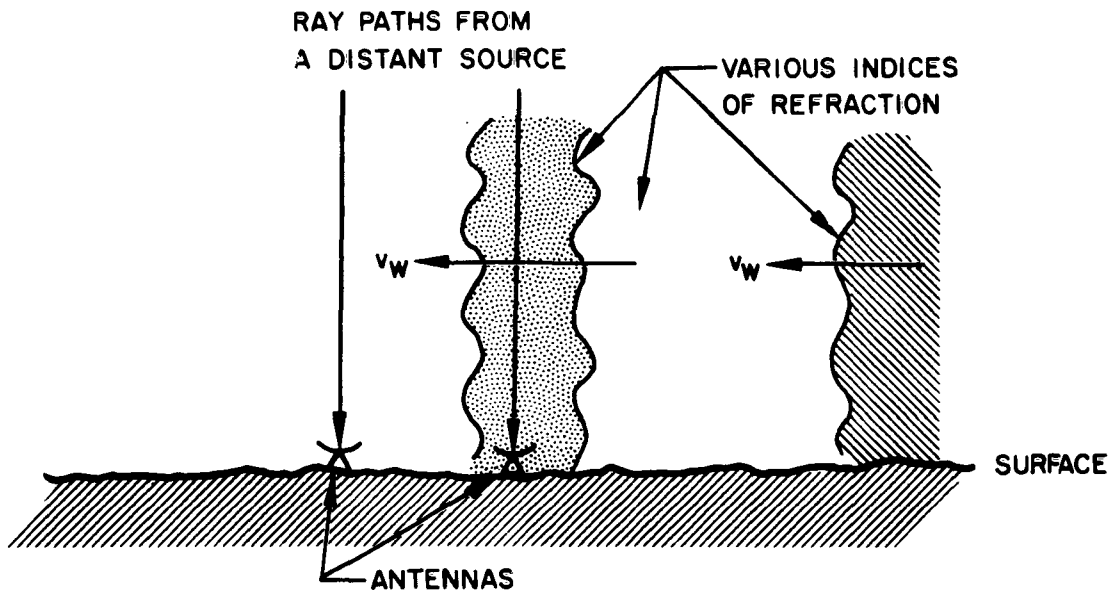

Fig. A-3 A Model for Tropospheric Inhomogeneities

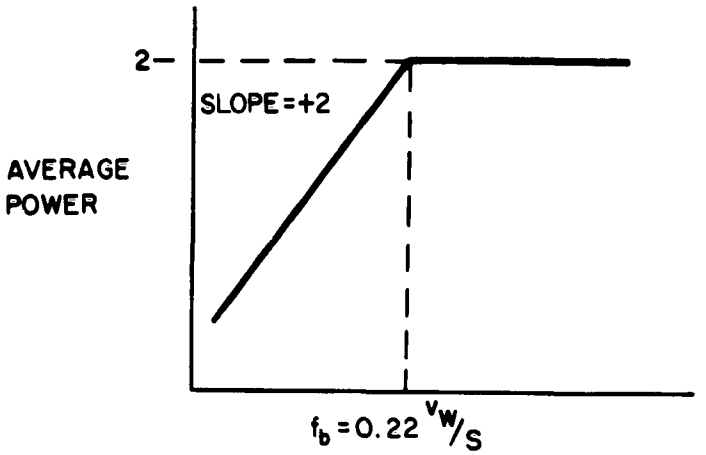

Fig. A-4 Effective Antenna-Separation Filter

equivalent angle errors of an interferometer system, these data provide the following results:

Antenna Separation (ft)	Extreme Angle Errors (mil)
500	±0.021
1,420	±0.016
1,920	±0.013

Deam and Fannin (Ref. 15) made similar measurements at the same location but at a different time and at 9,350 Mc. Their tests showed that there is only a slight increase in the rms phase difference when antenna distances are greater than 250 ft. Tests for several hours with 500-ft antenna separation showed an rms phase difference corresponding to an angular error of 0.007 mil rms.

Both the model used by Barton and the tests made by Thompson, Deam, and Fannin fail in several ways to represent the actual case. All tests were performed necessarily at low elevation angles and over paths which were only a few thousand feet above the terrain. Surface-induced atmospheric inhomogeneities were therefore more prevalent than they would be for an interferometer installation designed for tracking satellites and space vehicles.

An additional difference is the altitude itself. The propagation velocity varies according to the equation

$$c/v = 1 + \frac{77.6 \times 10^{-6}}{T} \left(P + \frac{4,810}{T} P_{wv} \right) \qquad \text{(A.8)}$$

where

c = propagation velocity in vacuum

T = temperature, °K

P = total pressure, mb

P_{wv} = pressure of water vapor present, mb

The fractional changes of velocity compared to vacuum is plotted in Fig. A-5 as a function of altitude for a standard atmosphere (Ref. 11). At an altitude of 30,000 ft, the velocity change is 1/3 of its sea-level value and at an altitude of 55,000 ft the velocity change is 1/10 of the sea-level value. Therefore, in addition to becoming more homogeneous with increasing altitude, the atmosphere is also incapable of causing as large a variation in velocity. A major contributor to atmospheric anomalies is humidity. The velocity change omitting the humidity term is also given in Fig. A-6. Contributions to changes in velocity due to water vapor are seen to be negligible above 20,000 ft.

Barton's model appears to have some validity when applied to the higher frequency components of spectral density of range variation. It seems reasonable to imagine

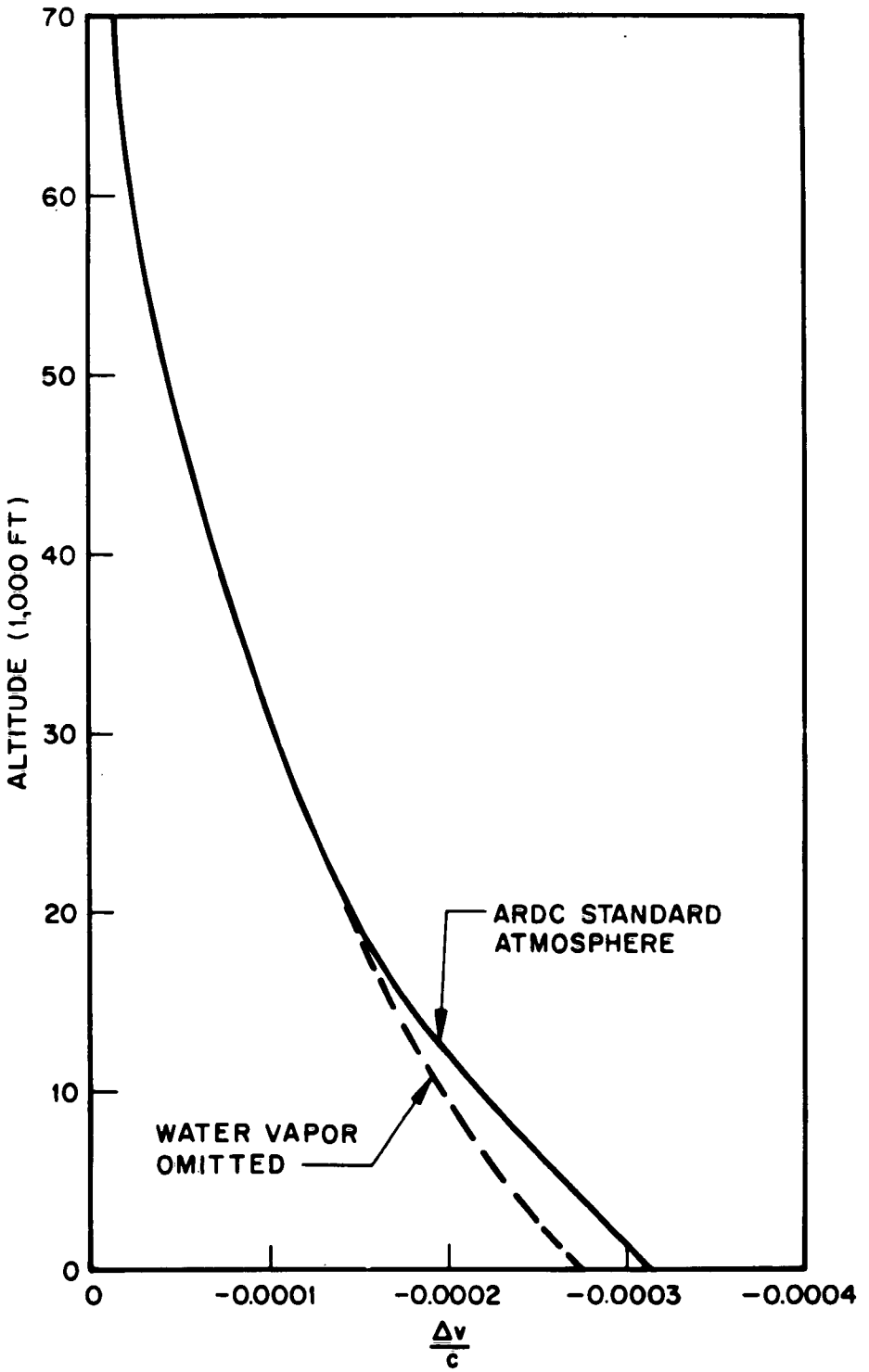

Fig. A-5 Fractional Change in Propagation Velocity Relative to Vacuum

various-sized globs of hot or moist air rising through cooler air and being blown about by winds. The lower frequency components of spectral density of range variation seem more likely to be caused by some mechanism which affects both interferometer ray paths simultaneously, and thereby causes no angular error. Daily and seasonal temperature variations are of this variety. Possibly, variations with periods of minutes and hours may be caused by a simultaneous buildup or dissipation of cumulus clouds over large areas; again, these variations would affect both paths simultaneously. The data described in Ref. 12 seem to suggest this conclusion.

The selection of a site for a precise interferometer has a large effect on interferometer errors because of atmospheric anomalies and errors of v at the site. Equation (A.8) and Fig. A-6 suggest that the sites should be located at a high altitude in a climate which is dry, clear, calm, and temperate.

A.4 ANGULAR ERRORS DUE TO IONOSPHERIC AND TROPOSPHERIC BENDING

Ionospheric bending varies inversely as the square of the frequency. For $f = 1,000$ Mc and a target at 300-km altitude and 20 deg elevation angle, the average bending is about 0.08 mil (Ref. 16). Unfortunately, the variation of the electron density which causes this bending is quite large. The probable error in predicted bending at this frequency is about ± 0.04 mil. It appears that a suitable correction can be made with the multiplication of the average bending by $f_c^2/36$, where f_c is the critical frequency (in Mc) determined by ionospheric sounding.

The use of a higher frequency, i.e., $f = 2,300$ Mc, results in ionospheric bending of 0.015 mil, ± 0.0075 mil. In this case, the average correction is sufficient.

Tropospheric bending is considerably larger, on the order of 0.8 mil at 20 deg elevation. For targets well above the atmosphere, a correction of the form

$$\phi = \frac{n_o - 1}{A + B \tan \theta} [1 - Ch^{-D}] \qquad (A.9)$$

may be used to correct for the tropospheric bending (Ref. 17). The values of A, B, C, and D are obtained for the particular site and optimized for the range of θ to be used. For an angular error less than 0.01 mil at an elevation angle of 20 deg, the fractional change of propagation velocity $(n_o - 1)$ must be known to an accuracy of 10^{-2}. The same method used to determine v may be used for this correction. There is some doubt as to the accuracy of the correction. Reference 18 concludes that above 30 deg the error may be as low as 0.01 mil rms.

A.5 CONCLUSIONS

The various factors which affect the accuracy of precise radio interferometers are discussed in this appendix. Equations are developed which relate the angular errors to errors of antenna spacing, local propagation velocity, and atmospheric anomalies. It is also shown that in a few cases the range must be known and its required accuracy is derived.

When all the factors are considered, it appears possible to obtain an angular accuracy on the order of 0.01 to 0.05 mil rms from interferometers with baselines of 2,000 to 10,000 ft.